NEWTONIAN AND ELASTIC LIQUID JET INTERACTION WITH A MOVING SURFACE

by

Bavand Keshavarz

B.Sc., Sharif University of Technology, 2008

A THESIS SUBMITTED IN PARTIAL FULFILLMENT OF

THE REQUIREMENTS FOR THE DEGREE OF

MASTER OF APPLIED SCIENCE

in

The Faculty of Graduate Studies

(Mechanical Engineering)

THE UNIVERSITY OF BRITISH COLUMBIA

(VANCOUVER)

April 2011

Abstract

In the railroad industry a friction modifying agent may be applied to the rail or to the wheel in the form of a liquid jet. In this mode of application the interaction between the high speed liquid jet and a fast moving surface is important. Seven different Newtonian liquids with widely varying shear viscosities along with twelve different solutions of polyethylenoxide (PEO) and water with varying relaxation times were tested to isolate the effect of viscosity and elasticity from other fluid properties. Tests for the Newtonian liquids were done with five surfaces having different roughness heights to investigate the effects of surface roughness. High speed video imaging was employed to scrutinize the interaction between the impacting jet and the moving surface. For both Newtonian and Elastic liquids and all surfaces, decreasing the Reynolds number reduced the incidence of splash and consequently enhanced the transfer efficiency. At the elevated Weber numbers of the testing, the Weber number had a much smaller impact on splash than did the Reynolds number. The ratio of the surface velocity to the jet velocity has only a small effect on the splash, whereas increasing the roughness-height-to-jet-diameter ratio substantially decreased the splash threshold. Moreover, the Deborah number was also salient to the splash of elastic liquids.

Preface

The authors of chapter 2 are Bavand Keshavarz, Sheldon Green, Martin Davy, and Don Eadie. Dr. Green found the need for an experimental work regarding the interaction of Newtonian liquid jets with a moving surface. I studied and determined the variables to be tested (liquid viscosity, elasticity, surface roughness and jet/surface speeds) and the experimental methodology with the supervision of Dr. Green. All the experiments were performed by me and the results were analysed with directions from my supervising committees Dr. Green, Dr. Davy, and Dr. Eadie. I wrote the manuscript with revisions and corrections from Dr. Green, Dr. Davy, and Dr. Eadie.

A version of chapter 2 has been published in a conference paper: **Keshavarz, B.**, Green, S.I., Davy, M.H., and Eadie, D.T., "Newtonian Airless Liquid Jet Interaction with a High Speed Moving Surface", accepted by the 23rd Annual Conference on Liquid Atomization and Spray Systems (ILASS Europe 2010), Brno, Czech Republic, Sep. 2010. Another version of the same chapter has been submitted to a relevant journal in this field.

The authors of chapter 3 are Bavand Keshavarz, Sheldon Green, and Don Eadie. Dr. Green identified the need for further testing regarding the effects of liquid elasticity on jet impaction over a moving surface. I determined the variables to be tested (liquid elasticity and relaxation times, and surface/jet speeds) with the supervision of Dr. Green. I did all the experiments and finished the data analysis with guidance from Dr. Green and Dr. Eadie. The manuscript was written by me with revisions and corrections from Dr. Green and Dr. Eadie. A version of chapter 3 is submitted to another relevant journal in this field.

Table of Contents

List of Tables

List of Figures

Glossary

D	Diameter [m]
R	Radius [m]
V	Velocity [$m.s^{-1}$]
V_n	Normal Velocity [$m.s^{-1}$]
V_t	Tangential Velocity [$m.s^{-1}$]
$V_{rel.}$	Relative Velocity [$m.s^{-1}$]
Re_n	Reynolds Number Based on Normal Velocity
We_n	Weber Number Based on Normal Velocity
Re	Reynolds Number Based on Relative Velocity
We	Weber Number Based on Relative Velocity
α	Jet Impingement Angle in Solid Surface Frame of Reference [Rad]
σ	Surface Tension [$N.m^{-1}$]
ε	Roughness Height [m]
μ	Viscosity [Pa.s]
ν	Kinematic Viscosity [$m^2.s^{-1}$]
ρ	Density [$kg.m^{-3}$]
Wt	Weight
C_d	Discharge Coefficient
$\dot{m}$	Mass Flow Rate [$kg.s^{-1}$]
A_n	Nozzle Area [m^2]
h	Lamella Thickness [m]

L	Lamella Length [m]
A_n	Nozzle Area [m^2]
λ	Largest Relaxation Time [s]
De	Deborah Number
El	Elasticity Number
m	Separating Line Slope
Π	Dimensionless Number

Acknowledgements

I wish to acknowledge my supervisor Professor Sheldon I. Green not only for the technical assistance, but also for his guidance, learned advice, and personal support during my master project. Professor Green exemplifies the best qualities of the consummate teacher and mentor. It was a real honour and pleasure working with you.

I would like to express my sincere gratitude to Professors Martin H. Davy and Donald T. Eadie for their guidance as my co-supervisors. I also extend my thanks to Professor James Feng for his help on analysing the non-Newtonian results. Additionally, I would like to thank Professors Bushe and Feng for reviewing the manuscript and for the helpful advice as my committee members.

I extend my sincerest thanks to Dave Elvidge, Xin Lu, Johnny Cotter, Dr. Kevin Oldknow and other members of Kelsan® Technologies for providing their expertise and insight in the industrial application of liquid friction modifiers and guidance throughout the course of my research.

I would like to thank the Kelsan® Technologies and Natural Science and Engineering Research Council of Canada (NSERC) for their financial support of this project.

I would like to express my gratitude to my friends and colleagues Ali Vakil, Dan Dressler, Larry Li, Purushotam Kumar, Andrew Tetzel and other members of my research group for all their helps during the past two years. Works and helps of co-op students Chris Elvidge, George Sterling, and Abhishek Jain are much appreciated.

I would like to thank the complex fluid lab manager Sara Hormozi for her utmost kindness and also for her helpful hints during the rheometry tests.

Special thanks go to my undergraduate advisers, Professor Kaveh Ghorbanian, Professor Reza Soltani, and my older colleague and dear friend Mehran Masdari for their great trust, kindness and support during my first steps in the science of experimental fluid mechanics.

Finally, it is my heartfelt pleasure to express my deepest gratitude to my parents and my beloved sister, without whose love, encouragement, and sacrifice none of this have been possible. I will remain eternally in their debt.

Dedication

Rose petals let us scatter
And fill the cup with red wine
The firmaments let us shatter
And come with a new design

If sorrow's soldiers incite
To shed lovers' blood tonight
With beloved I will unite
And his foundations malign

Hafez (14 A.D.)

To my Beloved Parents,

Saleh and Soghra

From whom I learned to live gleefully in the pursuit of science and love learning new ideas and designs.

Chapter 1: Introduction

1.1 Friction Control in the Railway Industry

The Canadian railway network, comprised of more than 72,000 kilometers of track through five time zones [1], annually transports more than 270 millions tones of freight. Rail transport is one of the most efficient and cost-effective forms of freight transportation in North America. With rising fuel costs making truck and air transport less efficient and with a continuing increase in population, railways will continue to increase their influence.

Due to this continuing economic influence, ongoing research is being followed by the industry into further improving the efficiency of rail transport. Railroads have recognized that by using an integrated approach to effectively managing the wheel-rail interface, significant benefits such as controlling wheel and rail wear and reducing fuel costs, can be obtained [35].

Recently, researchers have begun to focus their efforts on top of rail (TOR) friction control. Although it was discovered that TOR friction control significantly reduced fuel consumption [36], this is still a relatively new field as most of the world's railway industries still operate today without TOR friction management.

1.2 Liquid Friction Modifiers

One of the recent methods of TOR friction control is the application of liquid friction modifiers (LFM). Kelsan Technologies Corporation, located in North Vancouver, BC, is a leader in developing friction modifiers for the railway industry. Of particular interest is one of their LFM products known as KELTRACK HI-RAIL. The mentioned product is a water-based suspension

of polymers and inorganic solids showing non-Newtonian behavior [2]. This liquid is usually applied on the top surface of the rail through sprayers mounted on rail cars or locomotives [1]. Reduced fuel consumption, reduced rail/wheel wear and decreased lateral (curving) forces are some of the benefits of LFM utilization.

1.3 Current Application Methods of LFM's

In current practice in the railroad industry, air-blast atomizers transfer the LFM (atomized to form ligaments and droplets) to the rail surface. They are typically located a minimum of 75 mm from the top-of-rail surface in the case of application to the rail. Major issues in this application are the impaction of the liquid on the surface, and the interaction between the particles and cross-flowing air [3]. For effective deposition on the rail the droplets/ligaments should have sufficient velocity to avoid excessive deflection in the cross-wind, but not have such a high velocity as to cause splash or rebound after impaction. Both excessive deflection and splash would cause an undesirable reduction of transfer efficiency [4, 5]. To avoid the splash or rebound for the droplets/ligaments a study over the interaction between the falling droplets/ligaments and the moving or stationary surface is required.

1.4 Newtonian Droplet Impact on Stationary and Moving Surfaces

There are many studies in the literature of Newtonian droplet impact on a dry/wet stationary surface. Research done by Rein [6], Rioboo et al. [7], Yarin [8], and Deegan et al. [9] are good examples in this area. These authors have studied the effects of fluid properties such as viscosity, density, and surface tension on the post-impact outcomes. The impact of a single droplet on a dry surface was classified by Rein [6] into three types: deposition or spreading, splash, and

bouncing. Rioboo [7] later expanded this classification to six possible outcomes: deposition, prompt splash, corona splash, receding break-up, partial rebound, and complete rebound. Range et al. [10] and Crooks et al. [27] have studied more specifically the effects of surface roughness on the impaction outcome and have shown that surface roughness decreases the splash threshold significantly. More detailed results about Newtonian droplet impact on a dry solid stationary surface can be found in recent reviews by Yarin [8] and Deegan [9].

The impact of a droplet on a moving surface is also of interest in many industrial applications. Mundo et al. [12] studied the impact of a Newtonian droplet on a moving substrate and concluded that the tangential velocity of the droplet, in the frame of reference of the solid substrate, is less important than the normal component of droplet speed. In contradiction to their finding, several authors (e.g. Pavarov et al. [13], Courbin et al. [14], Okawa et al. [17], and Fathi et al. [18]) have reported that the tangential speed plays a significant role and include it in their splash/deposition criteria. Pavarov et al. [13] studied the case of impact on a spinning disc and observed that the air boundary layer, caused by the tangential velocity of the disc, lifts the droplet from the surface. Courbine at al. [14] and Bird et al. [15] found that asymmetric splashes occur on impaction of a droplet on a moving dry surface; in the frame of reference of the moving dry surface, the splash is strengthened in the downstream tangential direction of the impacting droplet and weakened in the upstream direction. In recent work Bird et al. [15] suggest a new physical model for the impact of a droplet on a moving surface. Their model highlights the interaction between the after-impact lamella and the moving surface [15, 16].

1.5 Non-Newtonian Droplet Impact

The widespread use of non-Newtonian liquids in industry has motivated many recent works studying the impact of a non-Newtonian droplet on a stationary/moving surface. Special attention has been paid to the behavior of elastic liquids. Bergeron et al. [11], Crooks et al. [27], Roux et al. [28] and Dressler et al. [3] report that elasticity helps in controlling the droplet deposition and inhibits splash. Bergeron et al. [11] showed in their experiments with polyethylene oxide (PEO) solutions that the high elongational viscosity of elastic liquids helped dampen the droplet's spreading after impact, preventing splash/rebound.

1.6 Coating through Jet Impingement

Recent experiments by Dressler [19] suggested that air-blast atomizers are less than ideal in transferring LFM to the rail top surface. The high speed atomizing air jet carried away some of the droplets/ligaments from the impacting surface, which leads to a lower transfer efficiency. To reduce this effect, a simple new airless, non-atomizing sprayer was developed at UBC. This sprayer produces a high-speed liquid jet that under some conditions does not break up. In contrast to the large amount of research done in the area of droplet impact on stationary/moving substrates, we know no studies of a high speed Newtonian or non-Newtonian liquid jet impinging on a high speed moving substrate.

1.7 Liquid Jet Impaction on Moving or Stationary Surfaces

Liu et al. [20] studied the interaction of a Newtonian liquid jet and a stationary substrate but were mainly concerned with heat transfer. A mathematical model has been proposed by Hlod et al. [21] to describe the interaction of a low speed highly viscous Newtonian jet with a slow moving surface. Since the speeds in their work were low, splash is not mentioned in their model.

1.8 Research Objectives

Little is known as to the effectiveness of application of these airless sprayers. In most spray coating applications the common method is liquid atomization but in the current study a continuous liquid jet is impacting on the rail surface. The primary objective is to achieve the best possible transfer efficiency (i.e. percentage of total liquid sprayed that remains on the target surface) while providing a uniform deposition on the target surface. Thus, it is desirable to understand sprayed liquid jet behavior both before and after potential impact occurs on TOR surface. Any liquid not reaching the surface or not remaining on the surface after impact will contribute to undesirable product wastage.

The main research objective of this project thus is to study the interaction of a non-Newtonian/Newtonian liquid jet with a rail surface, in the presence of a relative velocity. Although the physics associated with field application (i.e. moving spray nozzle over stationary rail) are not able to be exactly replicated in the lab, an accurate indication of spray-rail interaction can be obtained using the experimental setup developed for this purpose (see Chapter 2). This includes a linear traverse, which fires a rail surface at high speeds underneath a stationary airless sprayer nozzle. High speed imaging is used to capture images of the liquid jet

impaction behavior on the surface of the rail. With achieving the above objective a more solid understanding of the physics behind airless spray coating applications can be obtained.

Although industrial LFM are highly non-Newtonian, the initial study focused on Newtonian liquid jet interaction with a moving surface, to avoid the greater complexity of the non-Newtonian case. Chapter 2 deals with results for the Newtonian liquid jet impactions.

In addition, due to a lack of literature pertaining to non-Newtonian liquid jet impaction on moving surfaces another set of experiments were competed for elastic liquids. Chapter 3 includes results for elastic liquid interaction with a moving surface.

In combining knowledge gained from both of these investigations, it is hoped that an optimal application method or chemical improvements of the LFM, with the highest transfer efficiency possible, can be achieved.

Chapter 2: Newtonian Liquid Jet Impaction on a High Speed Moving Surface[1]

This chapter includes a detailed description of all the experiments and results related to the study of Newtonian liquid jet impaction on a moving surface. Selected liquids and surfaces, details of experiments, results, and finally conclusions for this study are all covered within this chapter.

2.1 Materials and Methods

Seven different mixtures of water and glycerine were used as the Newtonian test liquids, to isolate the shear viscosity effects (Table 1). The fluid viscosity and surface tension were respectively measured by a HAAKE VT550 viscometer and a Du Noűy ring apparatus at a temperature of 25°C. The viscosity of these mixtures varied by three orders of magnitude but the values of surface tension and density were constant to within ±13%.

[1] A version of chapter 2 has been published in a conference paper: **Keshavarz, B.**, Green, S.I., Davy, M.H., and Eadie, D.T., "Newtonian Airless Liquid Jet Interaction with a High Speed Moving Surface", accepted by the 23rd Annual Conference on Liquid Atomization and Spray Systems (ILASS Europe 2010), Brno, Czech Republic, Sep. 2010. Another version of the same chapter has been submitted to a relevant journal in this field.

Table 1: The composition and properties of Newtonian test liquids at 25 C

Glycerin[wt%]	Water[wt%]	Viscosity[mPa.s]	Surface Tension[mN/m]	Density[g/cm^3]
0	100	0.9	72.1	1.00
50	50	5.1	68.8	1.13
65	35	12.5	67.5	1.17
75	25	28.0	67.1	1.20
80	20	46.7	66.6	1.21
90	10	154	61.9	1.23
99.5	0.5	806	61.9	1.26

An airless spray nozzle with an internal diameter of 648 μm was used to apply the test fluids to a rapidly moving projectile. The projectile used in this work had a 13mm thick polished steel surface, previously the top surface of an AREMA 136# rail, fastened to a wooden-base carrier for the impaction surface (Figure 1).

Figure 1: Projectile

To study the effects of surface roughness, five different grades of sandpaper with different average roughness heights were selected and attached on the top surface of the projectile (Table 2). The corresponding roughness height to jet diameter ratios fell in the range 0.02-0.65.

Table 2: The properties of different sand-papers used as rough surfaces

Sandpaper Surface Number	Grit Size	Average Roughness [micrometer]	Roughness Ratio
1	40	425	0.65
2	60	265	0.41
3	100	190	0.21
4	220	68	0.10
5	600	16	0.02

The projectile was fired by a high-speed linear transverse system (an air cannon) that was designed and built for similar experiments by Dressler [19]. Once the projectile leaves the air cannon barrel it passes beneath the spray nozzle. It then strikes an energy dissipation device and comes safely to a stop (Figure 2). The projectile speed can be varied, depending on the air

pressure in the air cannon tank, from very low speeds (less than 1 m/s) up to speeds as great as 90 Km/hr. The main benefits of this test configuration are that it permits us to vary the surface speed independent of the jet velocity, and guarantees that impingement always occurs on a dry surface. In other words, it is a good approximation to the rail surface coating process.

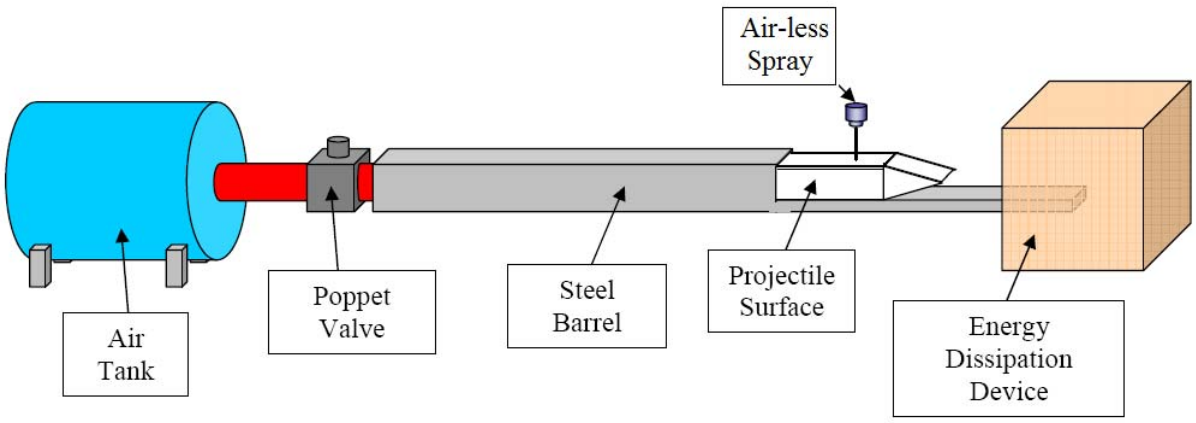

Figure 2: Experimental set-up, linear transverse system [19]

A Phantom V12 high speed video camera with a high-intensity halogen lamp for backlighting was used to visualize the jet impingement on the fast moving surface (Figure 3). The camera resolution was 800 x 1200 pixels with a frame rate of 6,200 pictures per second, and an exposure time of 9 microseconds.

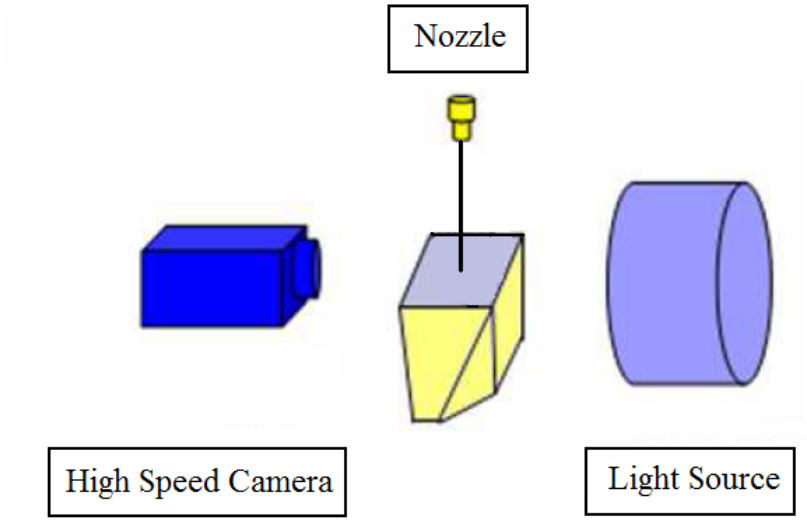

Figure 3: High Speed Camera and light source position relative to the projectile and the nozzle

The projectile velocity was measured through analysis of the high speed captured images. Jet diameter was measured using high speed magnified images of the jet at various heights from the nozzle exit. The captured images were then analyzed through an image processing code written in MatLab®. The jet diameter was measured at different nozzle back pressures and for different fluids. Mass flow rate measurements were done by weighing the liquid discharged from the nozzle over a span of 30 seconds. The average jet velocity was then obtained by dividing the mass flow rate by the fluid density and jet cross-sectional area.

2.2 Results and Discussions

Images were captured of the interaction between the surface and the liquid jet at different jet and surface speeds with various mixtures of water and glycerine. For all fluids tested, as the jet velocity increases (holding the surface speed constant) impingement transitions from direct deposition to splash. This finding is consistent with the single droplet impingement experiments of Yarin [5]. We also found that impingement transitions from direct deposition to splash while

keeping the jet velocity constant but increasing the surface speed, Figure 4. These findings prompted the authors to introduce the parameter of relative jet velocity, V_{rel}, which is the magnitude of the vector sum of the jet and surface velocities, Figure 5. The relative jet velocity was determined experimentally by vector addition of jet and projectile velocities.

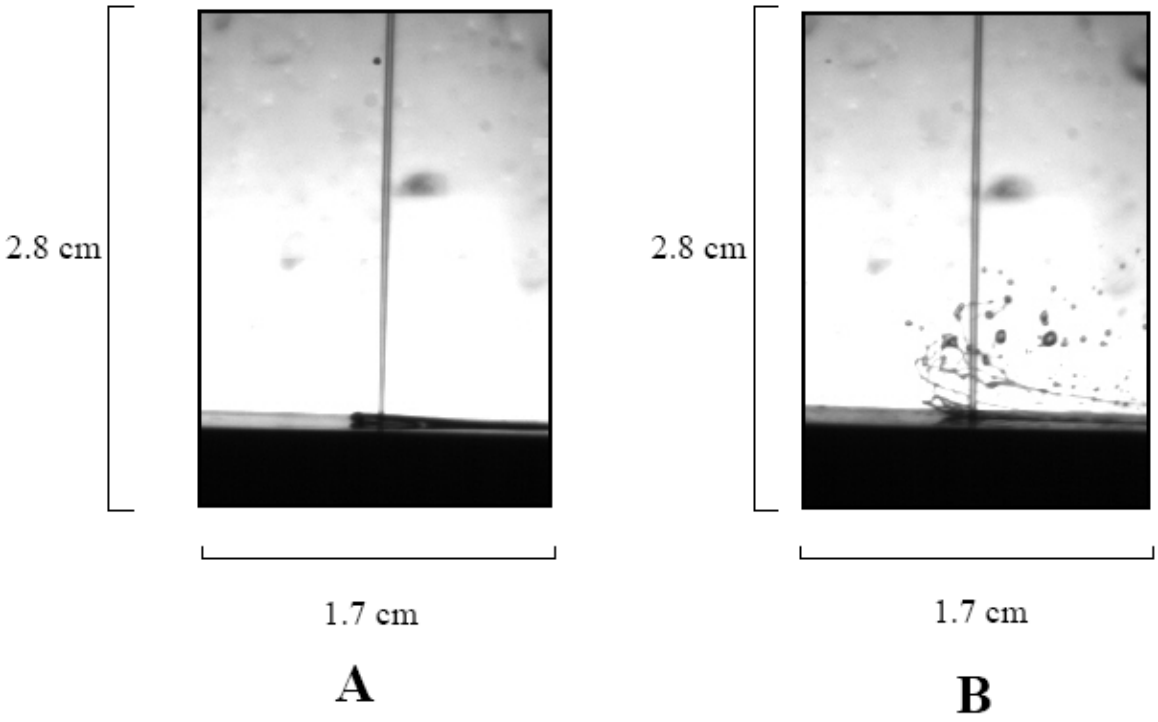

Figure 4: Projectile is traveling from left to right with a velocity equal to 3.2 m/s (A) and 8.9 m/s (B). In both (A) and (B) the Newtonian liquid jet velocity is 14.2 m/s.

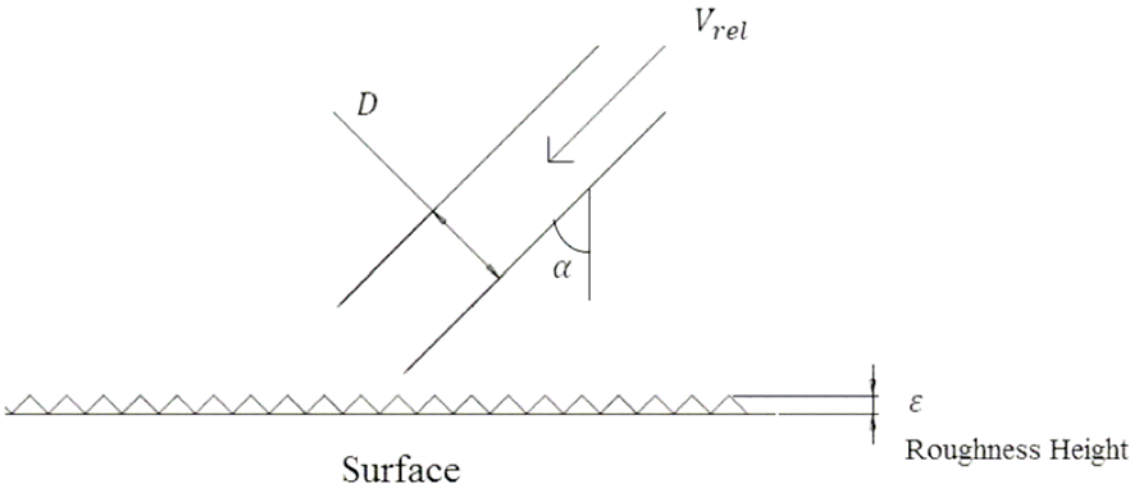

Figure 5: Relative Jet Velocity

Jet impingement of a Newtonian, non-cavitating liquid on a surface is a function of the relative jet velocity, (V_{rel}), the jet diameter, (D), the impingement angle in the frame of reference of the surface, (α), the fluid density, viscosity, and surface tension, (ρ, μ, σ), and the surface roughness, (ε)[2]. These seven variables may be reduced to four dimensionless groups:

$$\mathrm{Re} = \frac{\rho V_{rel} D}{\mu} \tag{1}$$

$$We = \frac{\rho V_{rel}{}^2 D}{\sigma} \tag{2}$$

α : Impingement angle in the frame of reference of the surface (3)

[2] It may also be a function of the surface material (e.g., as represented by the contact angle of a droplet on the surface), and the ambient air properties, but these effects are not considered here.

$\frac{\varepsilon}{D}$: Relative Roughness (4)

By adjusting the glycerine concentration (and thus the fluid viscosity), and simultaneously controlling the relative jet velocity, wide ranges of different Re and We numbers were achieved through our experiments (three orders of magnitude changes in Re number and almost one order in We).

One common way of characterizing flow rate behavior through a nozzle is by calculating the discharge coefficient at different Reynolds numbers. The discharge coefficient by definition is the ratio between the actual and ideal mass flow rate.

$$Discharge\,Coefficient: C_d = \frac{Actual\,Mass\,Flow\,Rate}{Ideal\,Mass\,Flow\,Rate} = \frac{\dot{m}}{A_n\sqrt{2\rho.\Delta P}} \quad (5)$$

The relationship between C_d and Re is depicted in Figure 6 The discharge coefficient has a small value at really low Reynolds numbers and rises to a nearly constant value between 0.8 and 0.9 at higher Reynolds numbers. This dependence is in accordance with the fact that viscous losses are more dominant at low Reynolds number than at higher Reynolds numbers. Lefebvre [22] has also reported a similar behavior for round orifices discharging in ambient gas. At still higher Reynolds numbers (around 600 for water + 65% glycerine by weight; around 1000 for water + 50% glycerine by weight) the discharge coefficient starts to decrease. This decrease is believed to be due to cavitation inception in the nozzle. Since the onset of cavitation is a strong function of local pressure and consequently velocity inside the nozzle, it can be expected that for liquids with lower viscosities (e.g. with lower amounts of glycerine in solution) cavitation

inception will occur at higher Reynolds numbers. Suh et al. [23] and Payri et al. [24] reported the same result in their experiments on liquids discharging from orifices into an ambient gas.

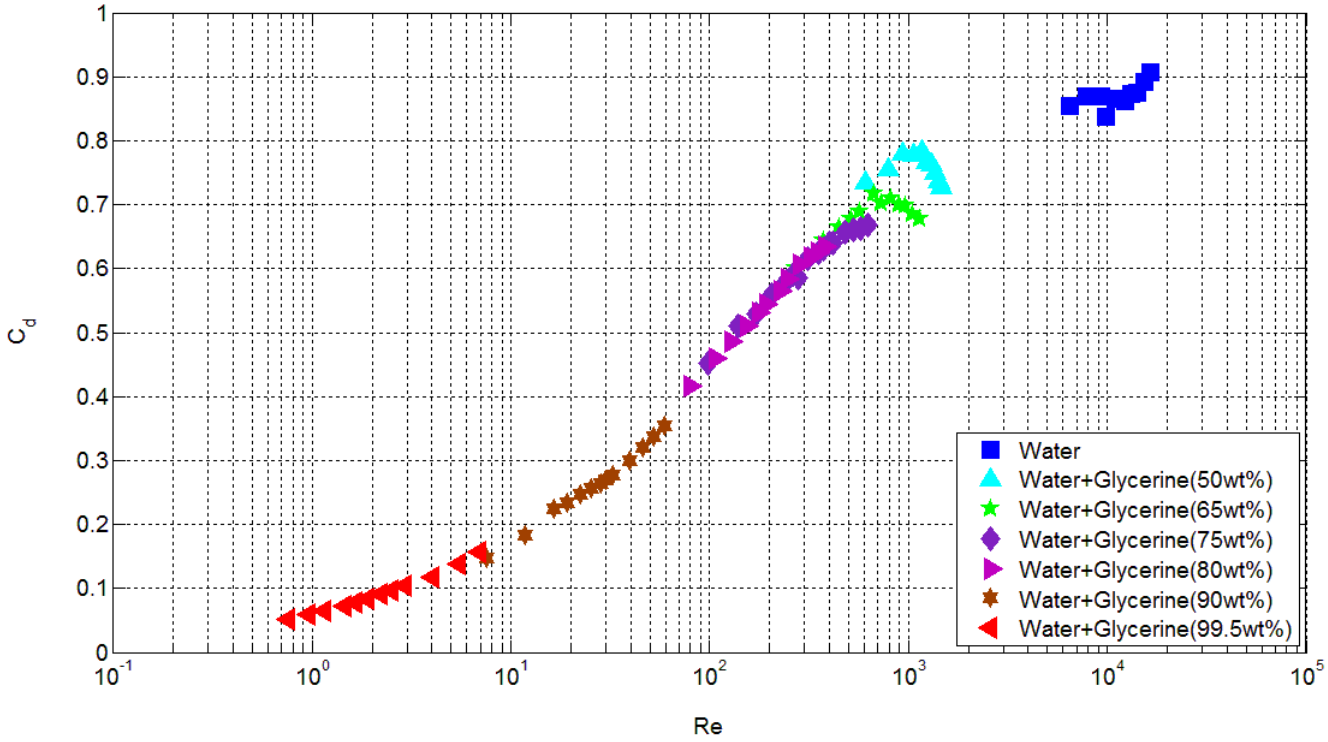

Figure 6: Discharge coefficient versus Reynolds number for different test liquids

Figure 7 shows the normalized jet diameter at the nozzle exit (normalized by the nozzle exit diameter, D_0) versus the Reynolds number for two different mixtures. It is interesting that up to 10% jet expansion occurs at very low Reynolds numbers. As the jet Reynolds number increases, the die swell diminishes until at high Reynolds numbers the contraction ratio becomes independent of Re and keeps a constant value near 0.87. These findings are consistent with the research of Middleman [25, 26].

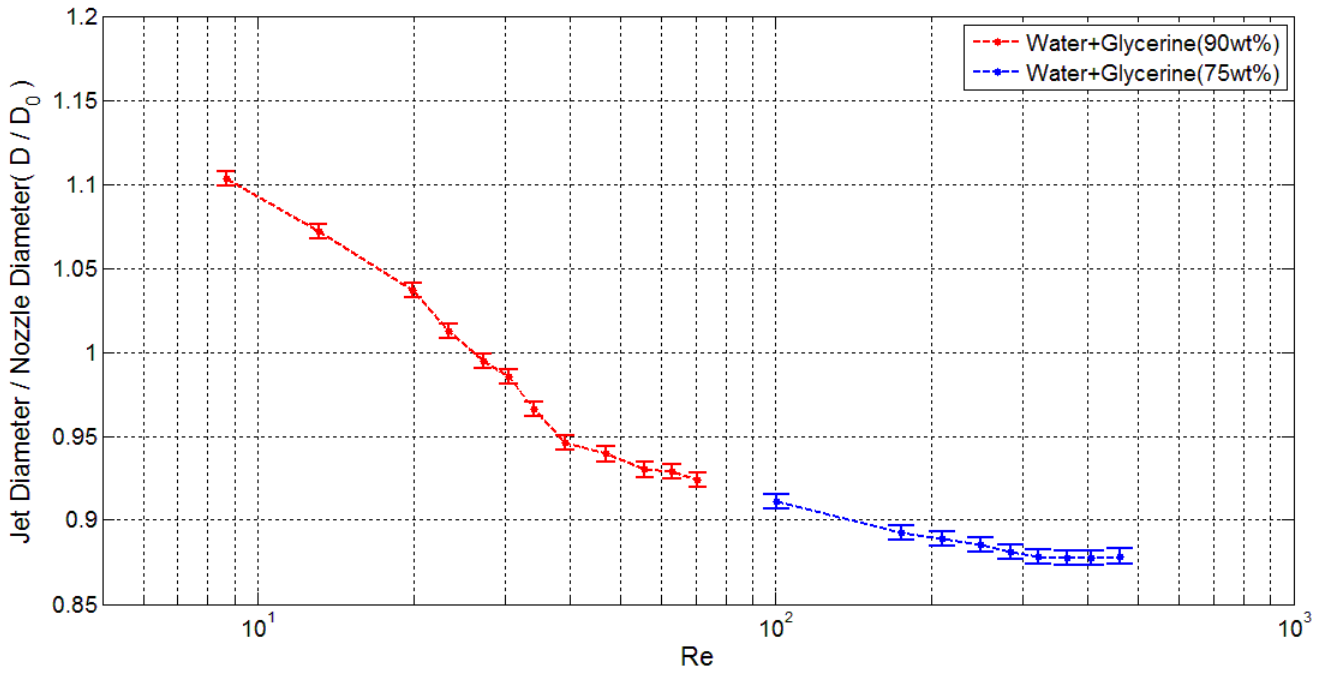

Figure 7: Normalized jet diameter versus Reynolds number at the nozzle exit

2.2.1 Smooth Surface

The splash/non-splash boundaries for Newtonian test liquids are depicted in Figures 8 and 9. From Figure 8 (see also Figure 14 for rough surfaces) it is apparent that the splash/non-splash boundary is much more strongly dependent on *Re* than on *We*. The lack of dependence on Weber number is perhaps not surprising in view of the very high ($200<We<2000$) Weber numbers studied here. As seen in Figure 9 (see also Figure 15 for rough surfaces), the effects of α on the splash are also modest relative to the effect of the Reynolds number. The critical Reynolds number above which splash occurs is about 350 for impaction on a smooth surface. Given that the Reynolds number used in this figure is based on the relative jet velocity, it is clear that the total impact energy is more important than its normal component. This finding is consistent with the insensitivity of splash to α, shown in Figure 9. It can be shown more

obviously if one considers the splash/non-splash results for a single fluid: Figure 10 shows the jet velocity versus surface speed for different splash/non-splash points for the water and (75%wt) glycerine mixture. The splash points are separated from the deposition ones by a constant relative velocity curve, i.e. $V_{rel} = 14.9\, m/s$.

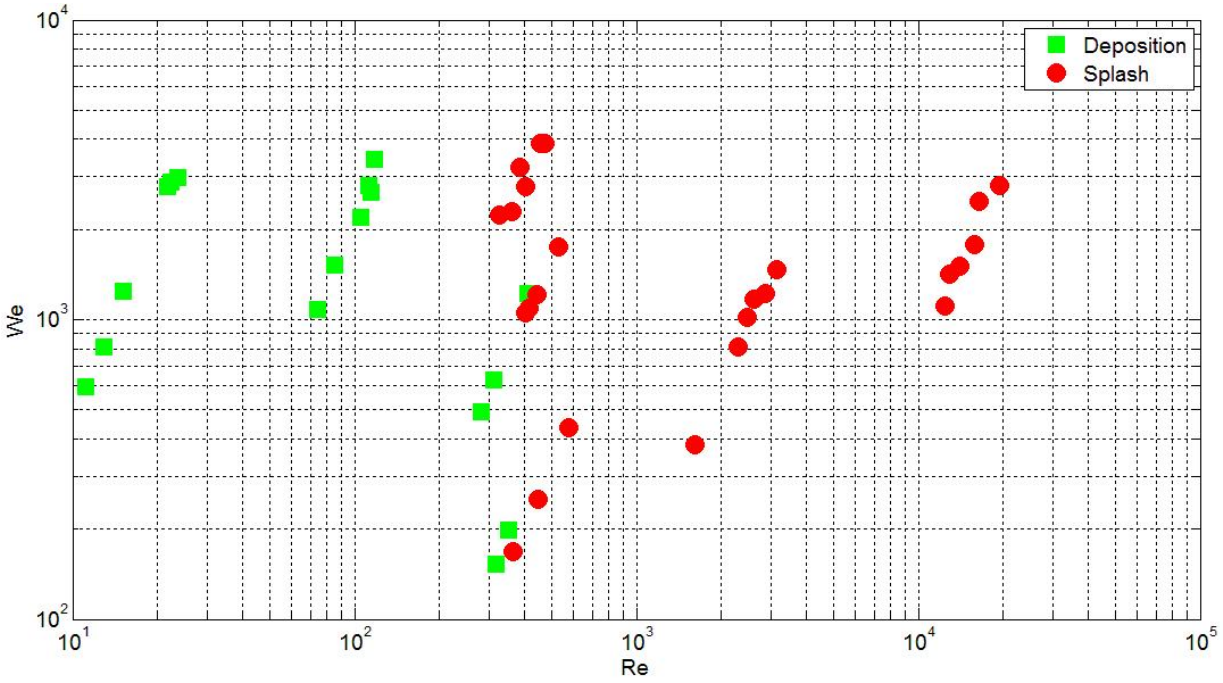

Figure 8: Splash/non-splash boundary for Newtonian liquid jet impact on a smooth surface (We vs. Re)

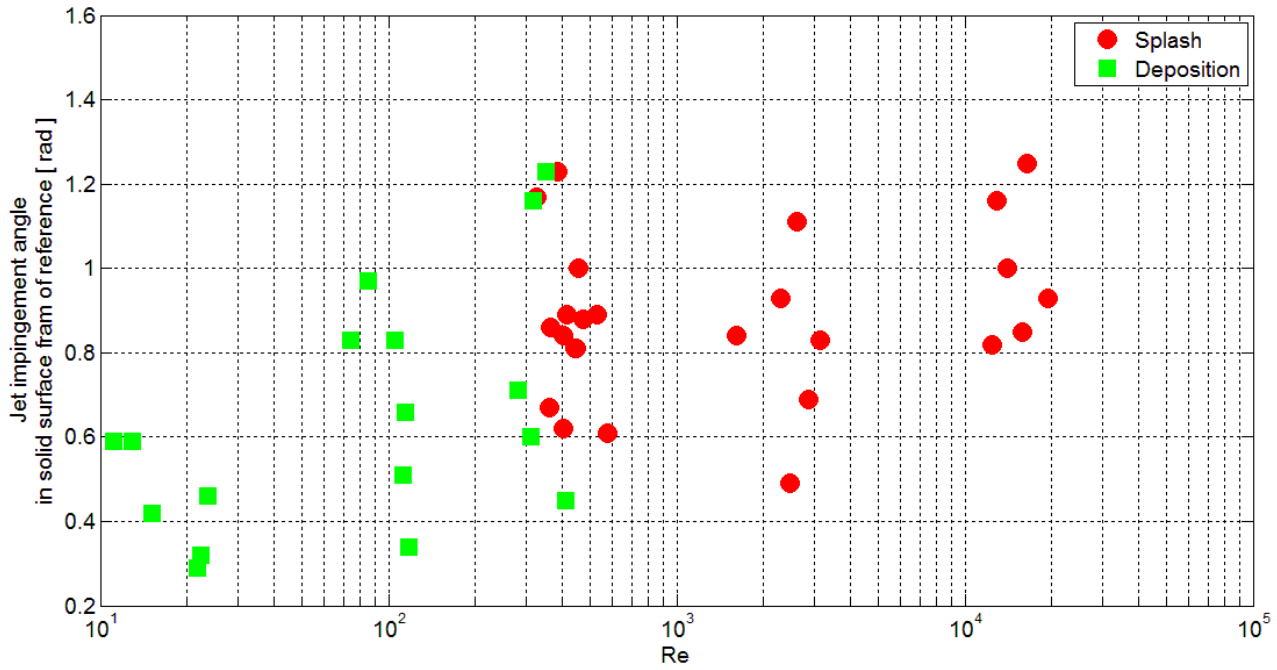

Figure 9: Splash/non-splash boundary for Newtonian liquid jet impact on a smooth surface (Jet angle vs. Re)

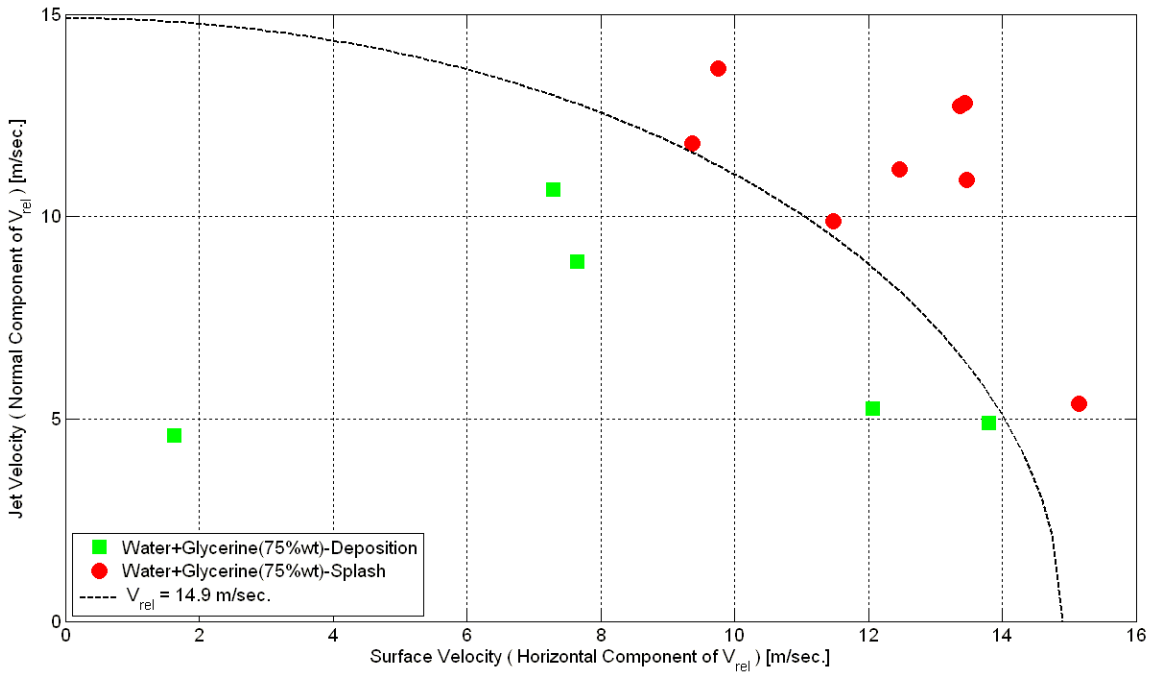

Figure 10: Splash/non-splash boundary for Newtonian liquid jet impact on a smooth surface (normal jet velocity vs. surface velocity)

2.2.2 A Model of Jet Impaction

Courbine et al. [14] studied droplet impact on a moving surface. They reported that when the impact results in splash, the splash pattern is asymmetric; in the frame of reference of the surface the splash is intensified in the downstream tangential direction of the droplet and diminished in the upstream direction.

This finding motivated Bird et al. [15] to develop a splash model that incorporates tangential speed. Figure 11 shows a schematic of their model for spherical droplet impact on a moving substrate. The lamella is originally the portion of the drop that has contacted the solid line (region *) and is transferred into an outward moving film with thickness h and length L. The normal speed of the droplet, tangential speed of the surface and the lamella are respectively V_n, V_t, and V_l. The relative kinetic energy will be $\rho\left(V_l - V_t\right)^2 L^2 h$ and the surface energy will scale as σhL. According to their model, splash occurs when the relative kinetic energy of the lamella is much greater than the surface energy:

$$\frac{\rho\left(V_l - V_t\right)^2 L}{\sigma} \geq C \gg 1, \tag{6}$$

where the constant value of C is a function of surface and air properties. This criterion explains the occurrence of the asymmetric splash observed by Courbine et al. [14]. To simplify and relate this criterion to the main dimensionless numbers, (i.e. Re, *We*, and relative angle or velocity ratio) several assumptions have been made in their modeling:

1. Conservation of mass dictates that the volume of droplets in the * and ** regions(identified in Figure11) are equal to each other.
2. The thickness of the propagating lamella is proportional to the momentum boundary layer thickness in the liquid, i.e. $h = c_1\sqrt{\nu t}$ where c_1 is a constant of order 1. The aforementioned assumption is widely used in modeling lamella thickness behavior; however, recent experiments by Ruiter et al. [16] have shown that the lamella thickness is a much more complex function of different parameters such as viscosity, time, droplet velocity, roughness, etc.
3. The critical time at which splash starts, t_c, corresponds to the moment at which the lamella distinctively separates from the drop. This criterion leads to the approximation $L(t_c) \approx a(t_c)$, which then gives t_c the value $\frac{\nu}{V_n^2}$.

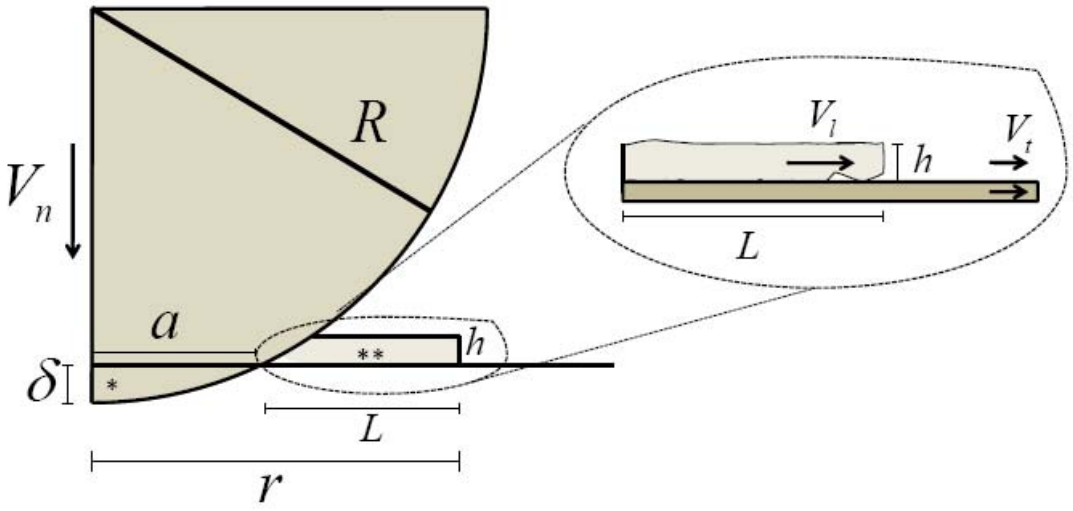

Figure 11: Model described by [15] for spherical droplet impact on a moving surface. The droplet is has a normal speed, V_n, and the substrate moves to the right with a speed equal to V_t.

The final splash criterion in terms of dimensionless numbers based on the normal droplet velocity for this model is expressed in [15] as

$$We_n \,\mathrm{Re}_n^{\frac{1}{2}} \left(1 - k\frac{V_t}{V_n}\mathrm{Re}^{-\frac{1}{2}}\right)^2 \geq K \tag{7}$$

where $We_n = \frac{\rho V_n{}^2 R}{\sigma}$, $\mathrm{Re}_n = \frac{V_n R}{\nu}$ and K and k are scaling factors (for their experiments they have values respectively equal to 5700 and 2.5).

Their criterion for droplet splash on moving substrates can be easily simplified and re-expressed in terms of dimensionless numbers based on the relative velocity ($V_{rel.} = \sqrt{V_n{}^2 + V_t{}^2}$) as

$$We.\mathrm{Re}^{\frac{1}{2}} \cos(\alpha)^{\frac{5}{2}} \left(1 - 2.5\,\mathrm{Re}^{\frac{-1}{2}} \tan(\alpha)\cos(\alpha)^{\frac{-1}{2}}\right)^2 \geq 5700 \tag{8}$$

where $We = \frac{\rho V_{rel.}{}^2 R}{\sigma}$, $\mathrm{Re} = \frac{V_{rel.} R}{\nu}$, and α is the relative impingement angle equal to $arc\tan\left(\frac{V_t}{V_n}\right)$.

A similar model and assumptions can be applied to the impact of a jet, instead of a droplet, on a moving substrate. Figure 12 shows the simplified geometry of a liquid jet column impacting on a moving substrate. The final criterion for jet impaction can be easily derived and expressed as

$$We.\cos(\alpha)^2 \left(\frac{1}{6c_1{}^2}\mathrm{Re}.\cos(\alpha) - \tan(\alpha)\right)^2 \geq 5700 \tag{9}$$

where c_1 is the scaling constant used in the lamella thickness expression ($h = c_1\sqrt{\nu t}$).

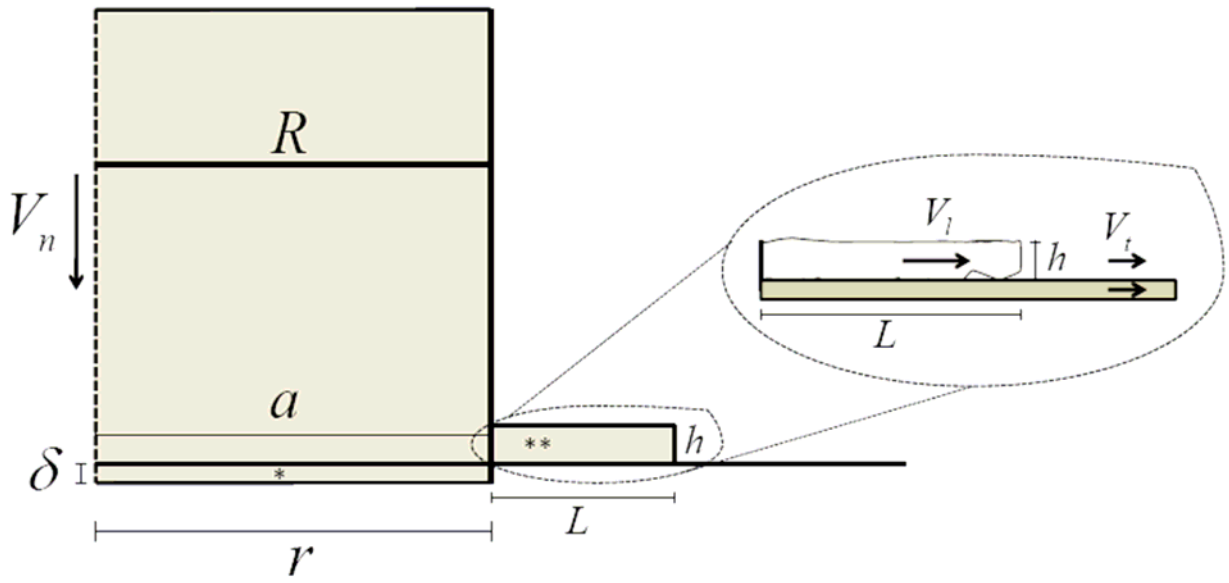

Figure 12: Model described by authors for cylindrical jet impact on a moving surface. The jet has a normal speed, V_n, and the substrate is moving to the right with a speed equal to V_t. The lamella is region ** having a thickness of h and length of L and moves outward with a speed equal to V_l.

Figure 13 compares the splash onset criteria for droplets and jets (equations 8 and 9). For both droplet and jet impaction, splash is relatively insensitive to the angle when α is near zero. It is also noticeable that the jet splash criterion shows a lower sensitivity to angle than does the droplet criterion. This trend agrees with our experimental results, shown in Figures 9, 10, and 15.

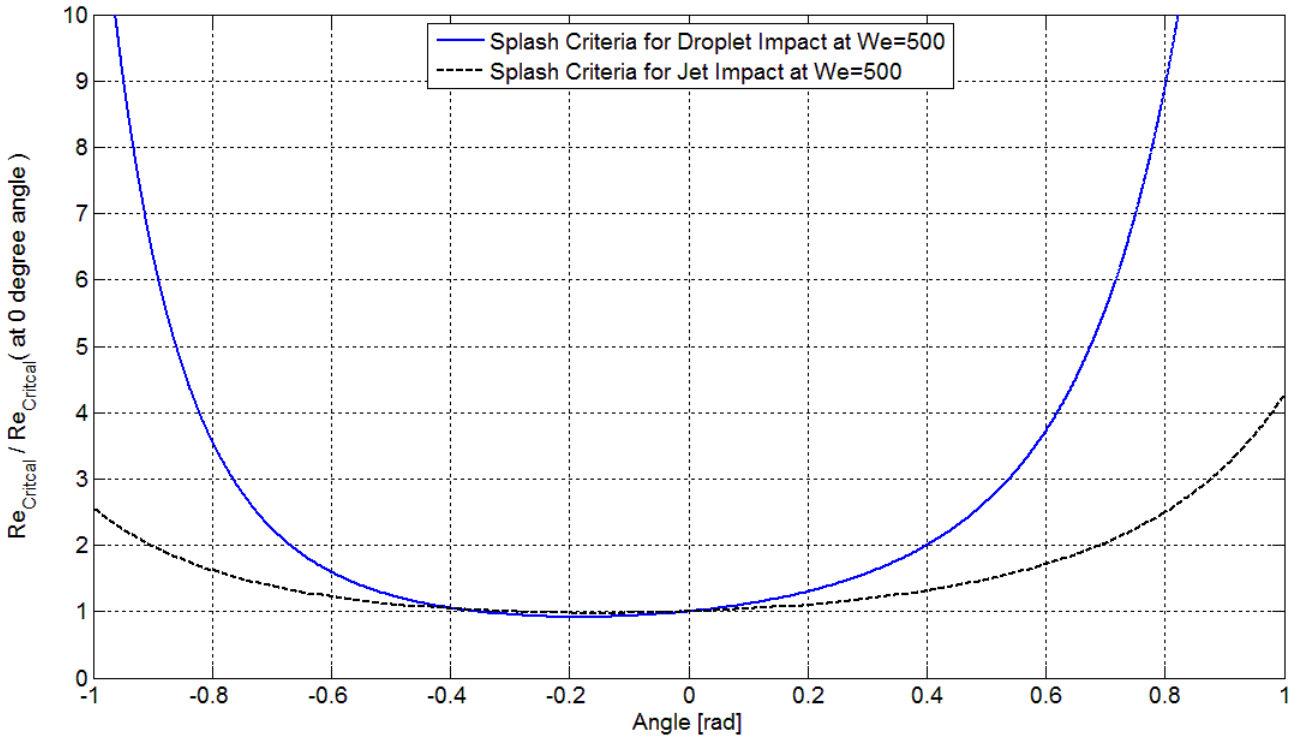

Figure 13: Comparison of splash criteria for drop and jet impact at a constant Weber number equal to 500.

2.2.3 Rough Surfaces

By attaching sandpaper with different average roughness heights to the moving surface we have studied the effect of impingement surface roughness. Interestingly, all five different roughness ratios show the same behavior found for the smooth surface, i.e. the most important parameter is the Reynolds number, not *We* or α. In this chapter we only show complete results for a roughness ratio equal to 0.21 (Figures 14 and 15- also results for other rough surfaces are shown in appendix A). For $\varepsilon / D = 0.21$ the critical Reynolds number has decreased to a lower value, around 60, relative to 350 for a smooth surface. The dependence of the critical Reynolds number on the roughness ratio is depicted in Figure 16; increasing the roughness decreased the critical

Reynolds number, which is in accordance with similar studies done on droplets [10, 27]. It can be observed that at lower roughness ratios (smoother surfaces) even a small increase in roughness ratio causes a significant decrease in the splash threshold but at higher values (rough surfaces) the splash threshold barely varies. Thus, the critical Reynolds number seems to decrease asymptotically to a constant value for larger roughness ratios. This finding is physically plausible because a thin jet (the lamella) striking a big obstacle (a roughness element) should experience splash onset for about the same conditions, whether the obstacle is 10 times the jet diameter or 100 times the jet diameter.

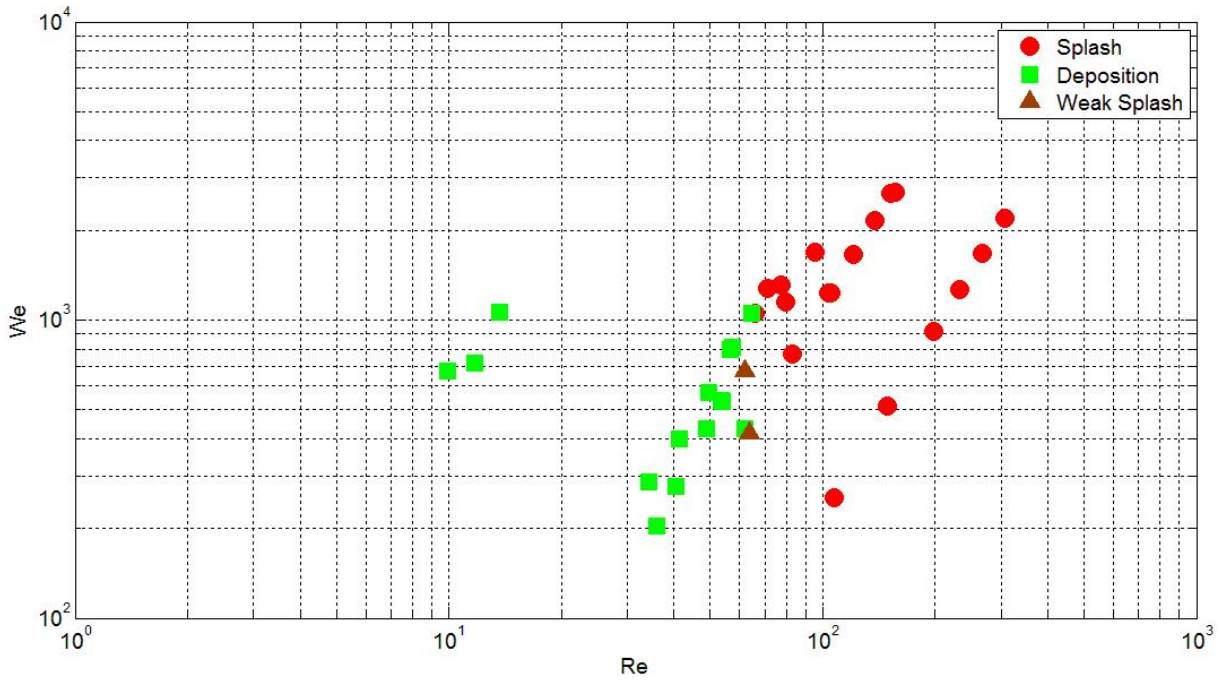

Figure 14: Splash/non-splash boundary for the surface with roughness ratio equal to 0.21

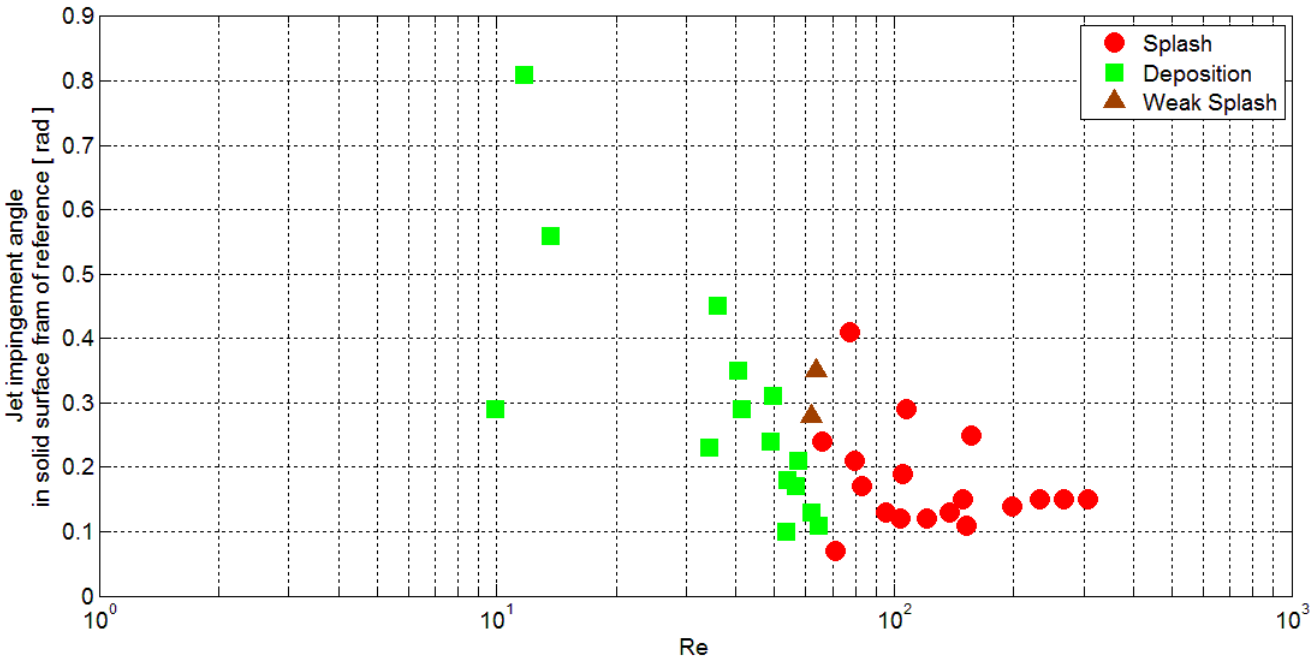

Figure 15: Splash/non-splash boundary for the surface with roughness ratio equal to 0.21

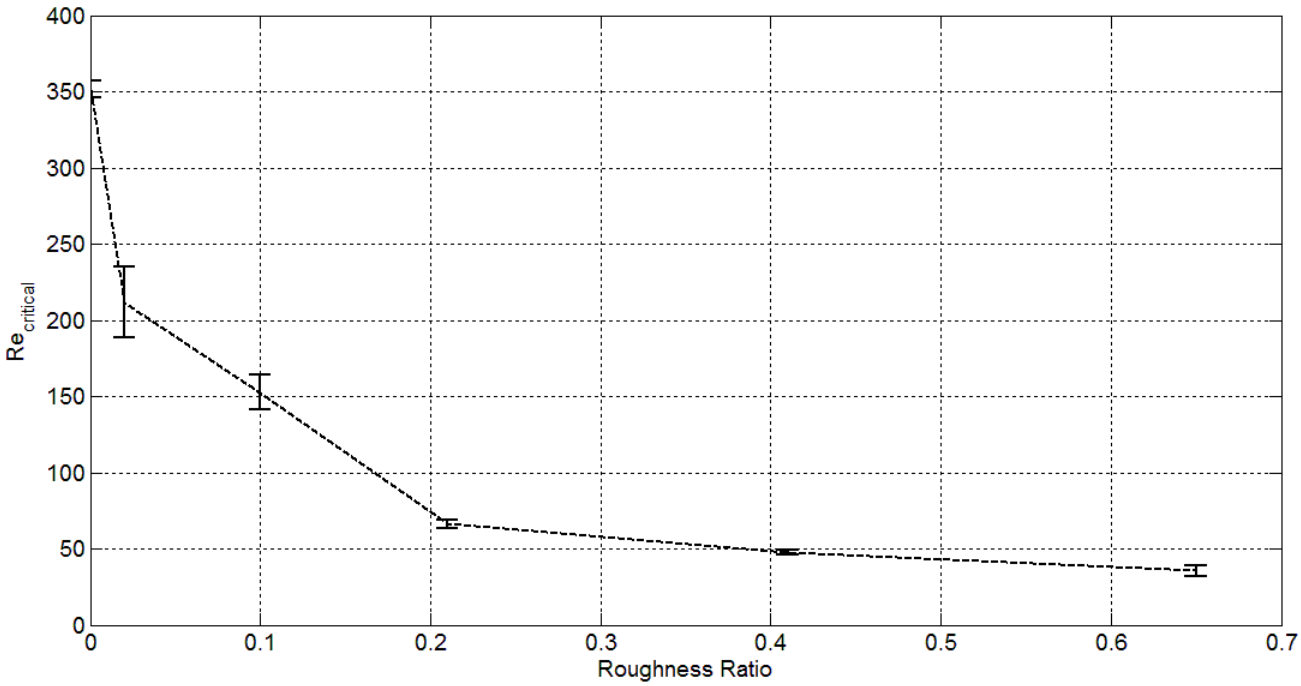

Figure 16: Critical Reynolds number versus roughness ratio

2.2.4 Conclusions

An experimental investigation into Newtonian jet impingement on a high speed moving surface with different roughness heights has been performed. The experiments are qualitatively consistent with previous studies of single droplet impaction and also provide new information concerning the impaction of liquid jets on smooth/rough moving surfaces.

The key findings of the present study are:

- Increasing the surface roughness ratio decreases the splash threshold and consequently decreases the transfer efficiency. The splash threshold is more sensitive to roughness ratio changes at lower roughness ratios (e.g. 0-0.1) than at higher roughness ratios (>0.1).
- For both smooth and rough surfaces splash is more influenced by Reynolds number, defined using the jet relative velocity, than by either Weber number or the ratio of the surface velocity to the jet velocity. This confirms that the total impact energy is more important than the energy associated with the normal component of velocity. It can also be concluded that for this flow the liquid's viscosity plays a more important role than the surface tension.
- A simple model is presented that predicts the dependence of jet splash onset on surface velocity. This model, which builds on the work of Bird et al. [15], is qualitatively correct in predicting that the jet impaction angle in the frame of reference of the surface should have only a modest impact on the onset of splash.

Chapter 3: Elastic Liquid Jet Impaction on a High Speed Moving Surface[3]

The authors could find no previous literature on the interaction of an elastic liquid jet with a moving surface. The current chapter builds on the previous chapter by exploring the effects of elasticity on liquid jet impaction on a moving surface.

For the impingement of a Newtonian, non-cavitating liquid jet on a moving surface the splash threshold is a function of the relative jet speed[4], (V_{rel}), the jet diameter, (D), the impingement angle in the frame of reference of the surface, (α), the fluid density, viscosity, and surface tension, (ρ, μ, σ), and the surface roughness, (ε)[5] [29]. These seven variables are reduced to four dimensionless groups:

$$\mathrm{Re} = \frac{\rho V_{rel} D}{\mu} \tag{10}$$

$$We = \frac{\rho V_{rel}{}^2 D}{\sigma} \tag{11}$$

α : Impingement angle in the frame of reference of the surface (12)

$\frac{\varepsilon}{D}$: Relative Roughness (13)

For the elastic liquids another variable will be added to our previous seven parameters. This new variable is the longest relaxation time, λ, of the PEO solution, which is a measure of its

[3] A version of chapter 3 is submitted to a relevant journal in this field.

[4] The relative jet speed is the magnitude of the vector sum of the jet velocity, V_j, and the surface velocity, V_s, i.e. $V_{rel} = \sqrt{V_j^2 + V_s^2}$ (Figure 4)

[5] It may also be a function of the surface material (e.g., as represented by the contact angle of a droplet on the surface), and the ambient air properties, but these effects are not considered here.

elasticity. This means that for the elastic liquids another dimensionless group including λ should be added. A widely used dimensionless parameter containing λ is the Deborah number:

$$De = \frac{\lambda V_{rel}}{D} \tag{14}$$

3.1 Materials and Methods

Twelve different solutions of water and polyethylenoxide (PEO) were used as the elastic test liquids, to study the effects of elongational viscosity (Table 3). The solution shear viscosity and longest relaxation time were respectively measured by a HAAKE VT550 viscometer and a HAAKE CaBER 1 extensional rheometer at a temperature of 25°C. For solutions with low elasticity (PEO solutions with lower molecular weights or concentrations) readings from the extensional rheometer were not accurate or repeatable. Hence, Rouse-Zimm theory (Doi and Edwards [30]) was employed to calculate the longest relaxation times in those cases. The relaxation time, which is a measure of elasticity, varied by four orders of magnitude for these mixtures. The fluid surface tensions were also measured by a Du Noűy ring apparatus at a temperature of 25°C; all surface tension values were close to that of water (72.1 mN/m), within a $\pm 5\%$ range.

Table 3: Testing elastic liquids

	Longest Relaxation Time (from CaBER)[ms]	Longest Relaxation Time (from Rouse-Zimm Theory) [ms]	Shear Viscosity [Pa.sec]
8000K PEO-0.5%wt	101.6	94.00	0.026
8000K PEO-0.1%wt	29.8	47	0.009
4000K PEO-0.5%wt	39	28.3	0.017
4000K PEO-0.25%wt	23.6	18.30	0.011
4000K PEO-0.075%wt	4.9	11.64	0.007
4000K PEO-0.1%wt	6.3	9.98	0.006
1000K PEO-1%wt	Not accurate	6.4	0.038
1000K PEO-0.5%wt	Not accurate	1.7	0.01
300K PEO-1%wt	Not accurate	0.21	0.009
300K PEO-0.5%wt	Not accurate	0.17	0.007
100K PEO-1%wt	Not accurate	0.028	0.007
100K PEO-0.5%wt	Not accurate	0.026	0.007

To generate the liquid jet, an accumulator was first filled with the elastic liquid. The accumulator is connected to a valve and a nozzle with an internal diameter of $648\,\mu m$. The accumulator is pressurized with nitrogen gas and a high speed liquid jet was created at the nozzle exit when the valve was opened. This jet impacted on a fast moving projectile. The projectile had a 13 mm thick polished steel surface (the top surface of an AREMA 136# rail) fastened to a wooden base carrier (Figure 1). To study the effect of surface roughness on impaction, sandpaper with a roughness height to jet diameter ratio of 0.1 was selected and attached to part of the top surface of the projectile.

The driving force for the projectile was an air cannon, which was designed and built for experiments done by Dressler [19]. After firing the projectile leaves the air cannon barrel and passes beneath the spraying nozzle. An energy dissipation device then stops the projectile (Figure 2). The projectile speed could be varied from less than 1 m/s to 25 m/s by changing the air cannon air pressure. This test set-up allowed us to vary the surface speed independent of jet velocity, and also guaranteed that impingement occurs on a dry moving surface, which is a good representation of the rail surface coating process.

For high speed imaging a Phantom V12 high speed video camera along with a high-intensity halogen lamp for backlighting were used (Figure 3), enabling the visualization of jet impingement on the fast moving projectile. Resolution of the camera and its frame rate were respectively set as 800 x 1200 pixels and 6,200 pictures per second; the exposure time was set at 9 microseconds.

The projectile speed could be easily measured by analysis of high speed captured images. Separate sets of high speed magnified images of the jet at different heights from the nozzle exit were captured for jet diameter measurements. They were analyzed by an image processing code written in MatLab® . Mass flow rate measurements of the discharged liquids were also done by weighing the liquid discharged from the nozzle over a span of 30 seconds, and then the average jet velocities were obtained by dividing the mass flow rate by the fluid density and jet cross-sectional area.

3.2 Results and Discussion

3.2.1 Flow Rates through the Nozzle

To find the jet velocity, flow rate measurements were completed for all twelve different PEO solutions. The flow of these elastic solutions through a circular nozzle is significantly different from the flow of simple Newtonian liquids. The latter case has been studied thoroughly in [22] and [29]. The single-phase Newtonian liquid discharge from a nozzle can be expressed by two dimensionless groups: Reynolds number and discharge coefficient which is defined as:

$$Discharge\,Coefficient: C_d = \frac{Actual\,Mass\,Flow\,Rate}{Ideal\,Mass\,Flow\,Rate} = \frac{\dot{m}}{A_n\sqrt{2\rho.\Delta P}} \tag{15}$$

However this common approach cannot be replicated for the discharge flow of elastic liquids since it neglects the elongational forces that are present in the flow (Boger [31] and Boger et al. [32]). Elongational forces can be considered, e.g. as proposed by Boger [31] and Rothstein et al. [33], by introducing other dimensionless numbers such as the Deborah number or the Elasticity number. The latter is defined to be the Deborah number over the Reynolds number:

$$El = \frac{De}{\mathrm{Re}} = \frac{\lambda\mu}{\rho D^2} \tag{16}$$

As mentioned by other researchers [31, 33], even considering the Deborah or Elasticity number effects does not completely explain elastic fluid behaviour at high Reynolds numbers. Consequently, most work has focused on very low Reynolds number flow (creeping flow) through nozzles/orifices (Rothstein et al.[33] and Cartalos et al. [34]).

To analyze the flow rate data from the current experiments with PEO solutions, we have followed the same approach used in many related works ([31], [33], and [34]); although those studies have been limited to the creeping flow regime.

In the current work the flow rate at a certain driving pressure difference across the nozzle was measured. From these data, and knowing the values of fluid viscosity and relaxation time from rheometry, one can easily calculate Reynolds, Deborah, and Elasticity numbers for this pressure difference. In previous work for Newtonian liquid impactions [29], numerous flow rate measurements with Newtonian liquids discharging from the same nozzle were made over a wide range of Reynolds numbers [29]. The current results were non-dimensionalized by dividing the pressure difference for a PEO sample by the equivalent pressure difference for a Newtonian liquid at a similar Reynolds number. Figure 17 is a summary of all the flow rate data for twelve different elastic solutions ranging from very water-like solutions, having negligible Elasticity number (5.7×10^{-4}), to less dilute mixtures, having a significant Elasticity number (10) and consequently elastic behaviour. For each liquid the normalized pressure difference is plotted versus Reynolds number. As could be anticipated, the normalized pressure difference is almost equal to one for very dilute and water-like solutions since they have negligible elasticity. For less dilute solutions the normalized pressure, which is always higher than one, first increases and then diminishes as a function of Re. It should be kept in mind that while increasing the Reynolds number, for a constant Elasticity value, the Deborah number is also increasing (equation 16). At low Reynolds number, as the jet velocity increases both the Deborah and Reynolds numbers increase. But, at these low Reynolds numbers elongational forces are large relative to inertial forces and significant additional pressure (relative to inelastic liquids) is required to overcome the elongational forces. At higher Reynolds numbers the inertial forces become more dominant

and the role of elasticity is diminished, so the driving pressure approaches that required for an inelastic liquid. The higher required pressures at lower Reynolds numbers and a reversion to more Newtonian behaviour at high Reynolds numbers has also been observed by other researchers [31], [33], and [34].

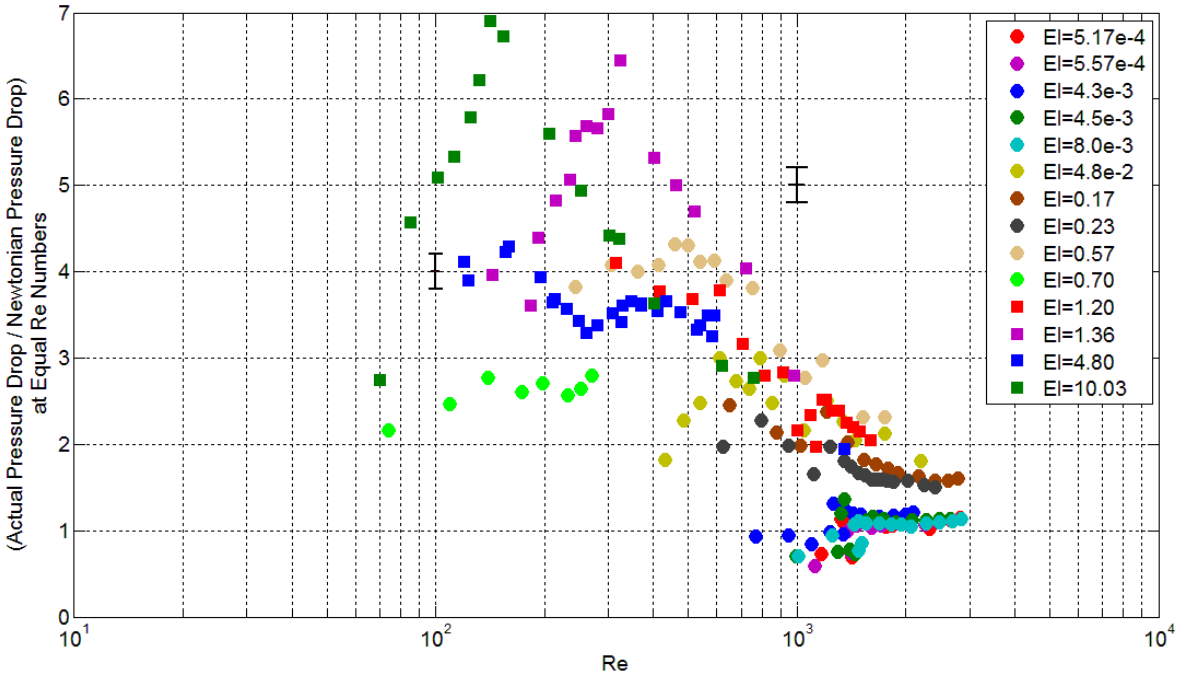

Figure 17: Actual pressure drop for elastic liquids over the Newtonian values at similar Re numbers vs. Re number.

3.2.2 Splash/Non-Splash Results

Figure 18 shows two photos of elastic liquid jet impaction. Figure 19 shows an equivalent pair of photos of Newtonian liquid jet impaction. For equal values of shear viscosity, adding elasticity led to significant improvements of the splash threshold in all the tested cases. Elastic/elongational forces were helpful in preventing splash as they increased the resistance of

the moving lamella to lift off and kept it attached to the moving surface even at high impaction speeds (see, for example, part A of Figure 18). When splash does occur, the splash of elastic liquids differed from Newtonian liquid splash. For example, a comparison of Figure 18(B) with Figure 19(B) shows that due to increased elasticity post-impact elastic droplets are much larger than post-impact Newtonian ones. Furthermore, in the elastic liquid cases thin films or ligaments connect the droplets together; these filaments do not exist in the Newtonian splash cases. Similar findings were reported about atomized droplet sizes for elastic liquids in [2] and post impact droplet sizes in the case of elastic droplet impact on a moving surface by [3].

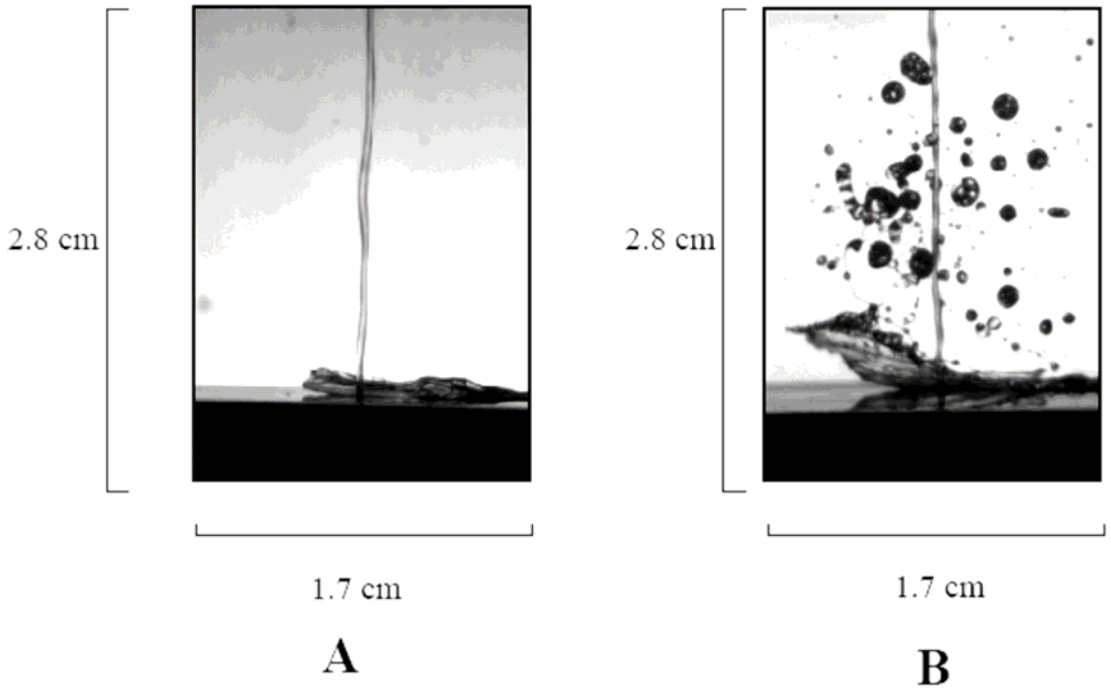

Figure 18: Projectile is traveling from left to right with a velocity equal to 5.9 m/s in both (A) and (B). The elastic liquid jet velocity is 20.3 m/s in (A) and 30.0 m/s in (B).

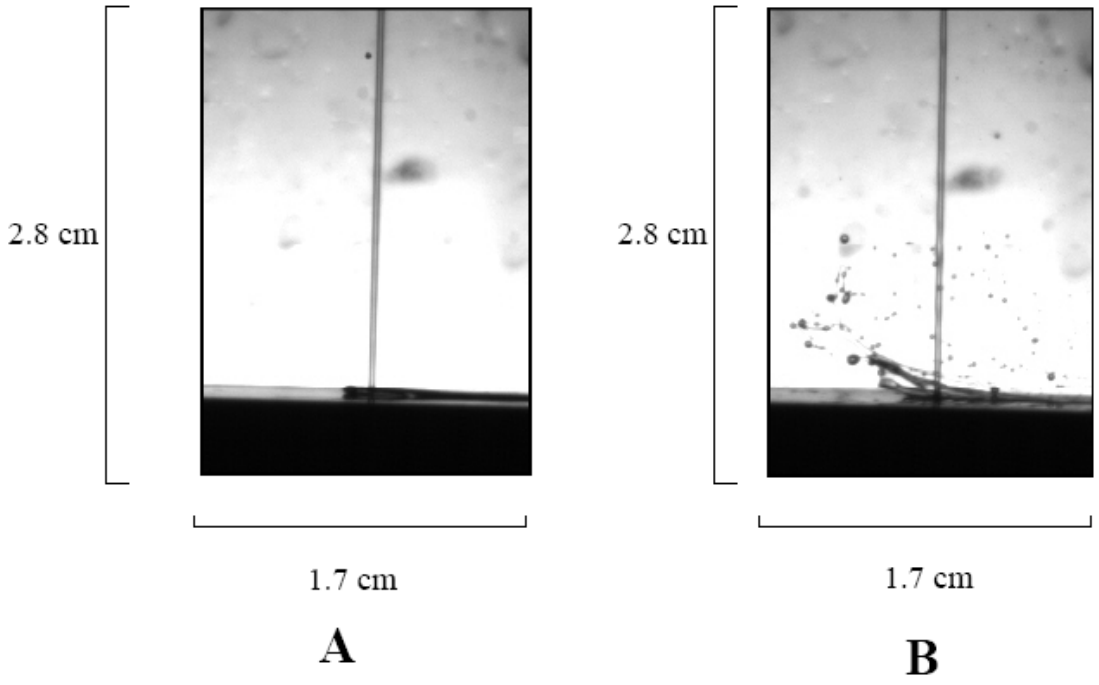

Figure 19: Projectile is traveling from left to right with a velocity equal to 3.6 m/s in both (A) and (B). The Newtonian liquid jet velocity is 12.5 m/s in (A) and 18.6 m/s in (B).

Figures 20 and 23 show the splash/non-splash data for elastic liquid jet impaction on smooth and rough surfaces in terms of Deborah and Reynolds numbers. In both graphs the line separating splash from deposition has a positive slope: 0.13 for the smooth surface and 0.081 for the rough one[6]. The positive slope of the separation line means that increasing the Deborah number causes the critical Reynolds number for splash to also increase. In other words adding elasticity to the liquid jet helps to avoid splash, which is in accordance with similar work done on droplet impact ([3], [11], [27], and [28]).

[6] The dependence of the slope of the dividing line on roughness ratio will be considered in follow-on work.

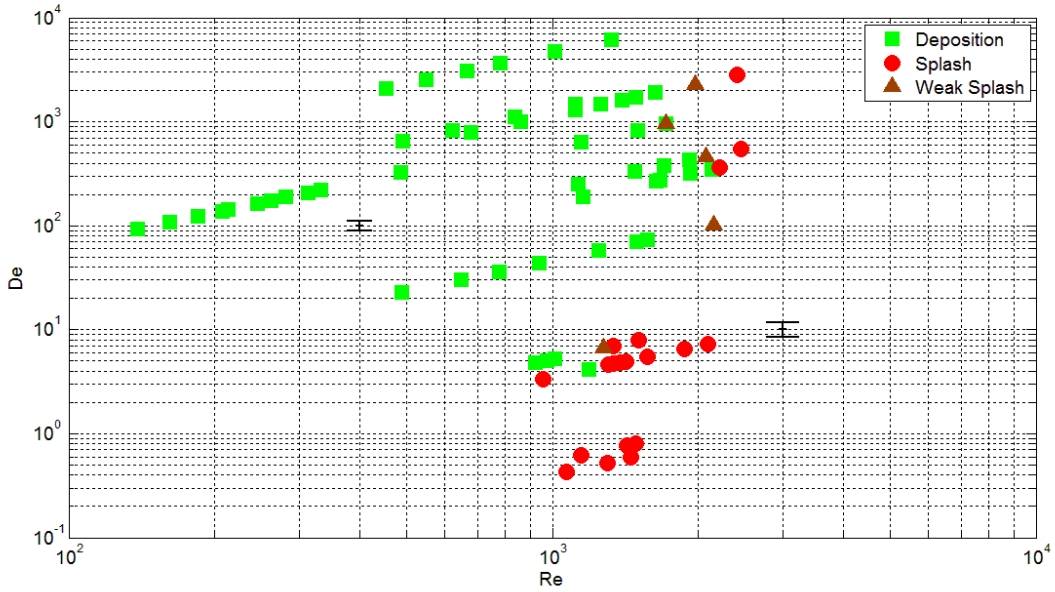

Figure 20: Splash/non-Splash boundary for elastic liquids impacting on the smooth surface

The importance of both Deborah and Reynolds numbers prompted the authors to define a new dimensionless number based on the separation line slopes, m, in Figures 8 and 11. The new dimensionless number is $\Pi = \frac{\mathrm{Re}}{De^{m}}$, with $m = 0.13$ for a smooth surface and $m = 0.081$ for a surface with roughness ratio 0.1 . Figure 21 is a plot of splash/deposition in $\Pi - We$ coordinates for the smooth surface. Since the separation line between splash and deposition is nearly vertical, we conclude that We has at most a small role in jet splash. Figure 22 is a plot of splash/deposition in $\Pi - \alpha$ coordinates. Once again the separation line is nearly vertical, implying that the effect of α is small. Figures 24 and 25 are the equivalents to Figures 21 and 22, but for the rough surface. The same conclusions may be drawn about the small effect of the We and α on splash. These new findings concerning the weak dependence of splash on We and α are in agreement with our studies of Newtonian jet impaction [29]. They also imply that the two most important parameters affecting elastic liquid jet splash are the Reynolds and Deborah

numbers, which suggests that the inertial, viscous and elongational/elastic forces are dominant in this flow.

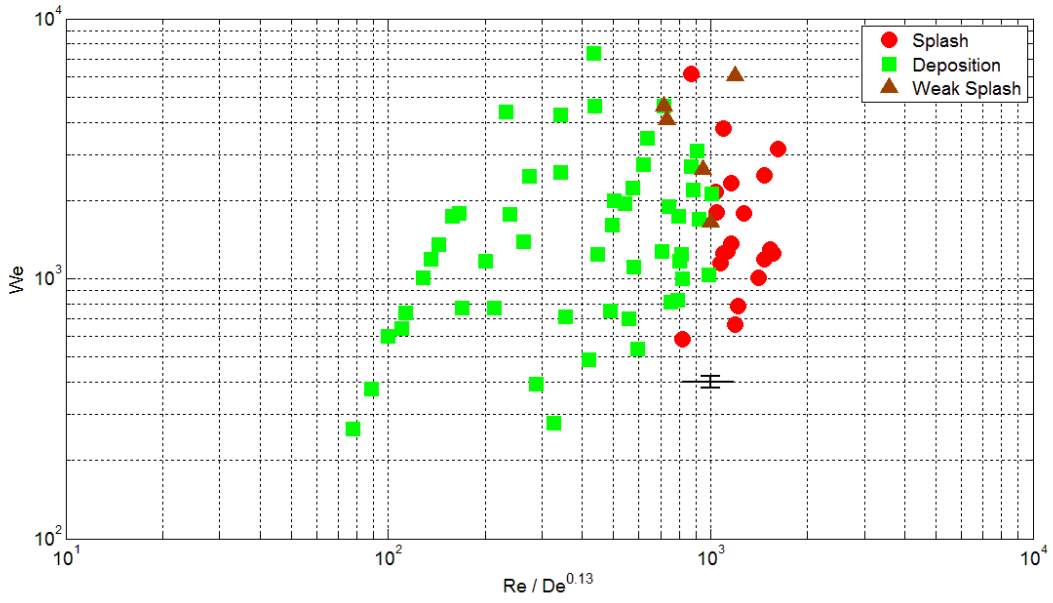

Figure 21: Splash/non-Splash boundary for elastic liquids impacting on the smooth surface

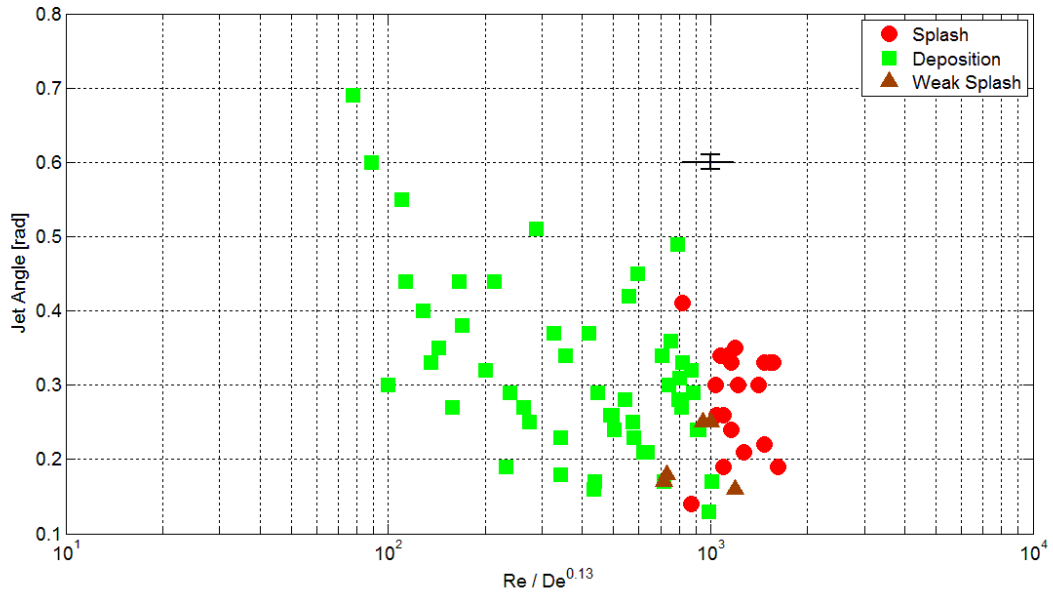

Figure 22: Splash/non-Splash boundary for elastic liquids impacting on the smooth surface

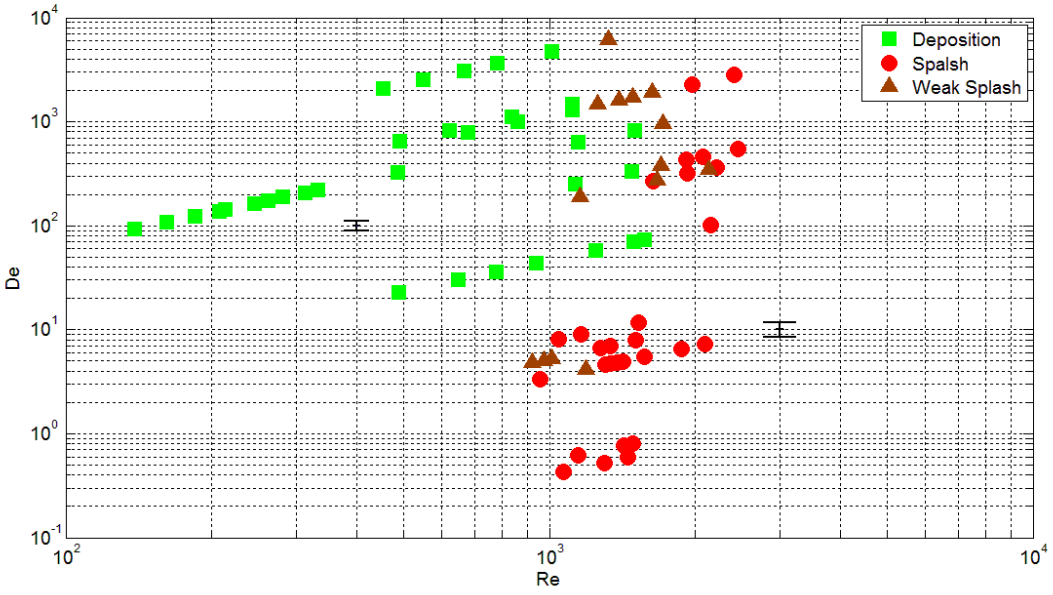

Figure 23: Splash/non-Splash boundary for elastic liquids impacting on the rough surface

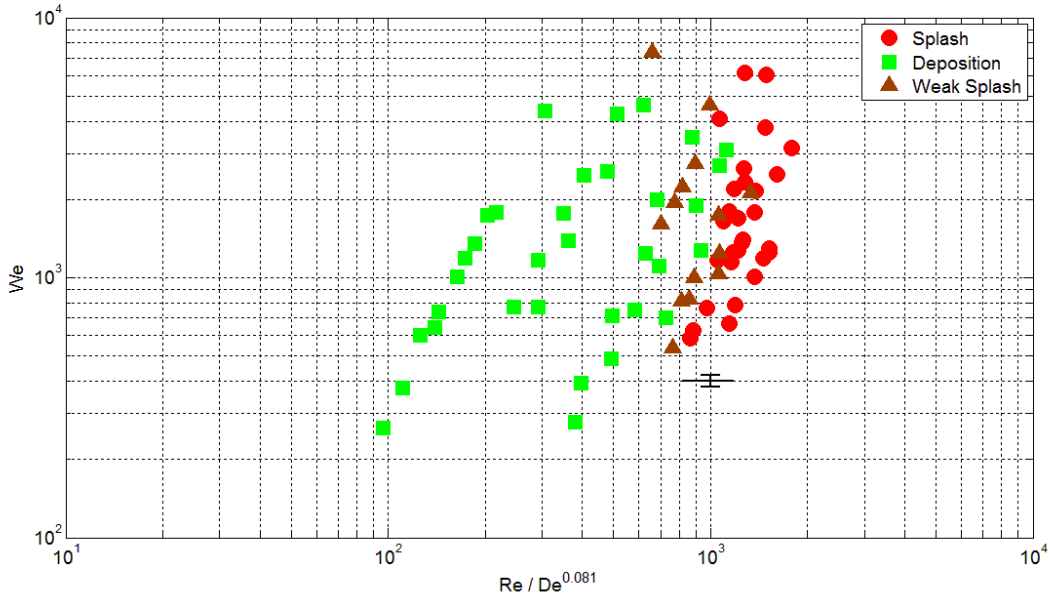

Figure 24: Splash/non-Splash boundary for elastic liquids impacting on the rough surface

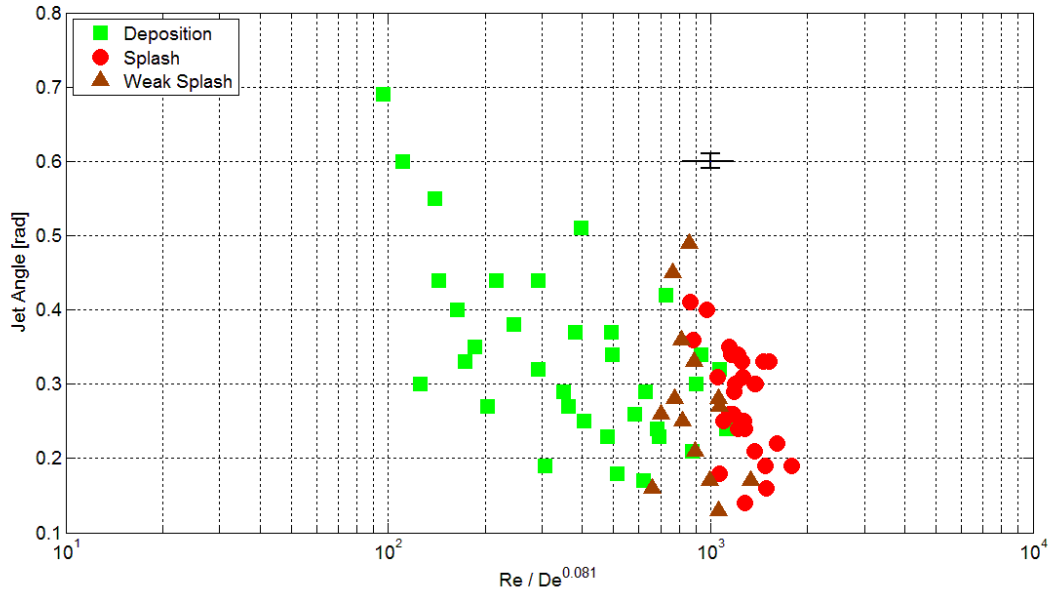

Figure 25: Splash/non-Splash boundary for elastic liquids impacting on the rough surface

3.2.3 Conclusions

Twelve different samples of elastic liquids (polyethylenoxide solutions) were prepared and tested in order to study the effects of elasticity in the liquid jet impingement on a high speed moving surface. The experiments and the results are qualitatively consistent with previous works of both single elastic droplet impaction and Newtonian jet impingement on a moving surface.

The key findings of this study are:

- Adding elasticity significantly increased the splash threshold relative to a Newtonian liquid of equal viscosity.
- For both smooth and rough surfaces the most important dimensionless numbers were the Reynolds and Deborah numbers.
- As was also the case for the Newtonian liquid jet impaction, the Weber number and jet relative angle play only a small role in impaction.

Chapter 4: Conclusions and Recommendations for Future Work

Using a pre-built experimental setup, the interaction of an airless sprayer and a moving rail surface were studied. High speed imaging was employed to capture the impaction of the jet on the moving surface.

Two sets of different experiments with Newtonian and elastic liquid jets were accomplished in order to study the interaction of a liquid jet with a moving surface. For the Newtonian liquids, tests were done with seven different mixtures of water and glycerine. Five different sandpapers with different roughness ratios were also selected in order to study the effects of surface roughness. For the elastic liquids, twelve different mixtures of polyethylenoxide (PEO) and water, with different maximum relaxation times, were tested in order to set aside the effects of elasticity.

4.1 Conclusions for Newtonian Jet Impaction

- Complete analysis of the experimental data for six different smooth and rough surfaces led to this fact that, for each surface, among the related dimensionless numbers the most important one is the Reynolds number. In contrast to the results reported by previous works about droplet impact, Weber number is not affecting the splash. However, one should not ignore this fact that the tested Weber numbers were always higher than 100. This means a high ration of inertial forces over the surface tension ones which can be a reason for the insensitivity of splash to surface tension and consequently Weber number.

- The impingement angle which represents the ratio of tangential velocity over the normal velocity was not playing an important role in determining the splash, in the range of

tested values which were mostly around zero, i.e. near to complete normal impact. This was in accordance with the previous experiments and models done about droplet impact. Based on previous models built for droplet impact, a new model was also developed for the liquid jet impaction and the model also predicted insensitivity of splash to jet relative angle for angles near to zero.

- Comparing results between 6 different smooth and rough surfaces, one can find that the surface roughness ratio showed a significant effect on splash criteria. Increasing the roughness ratio lead to a dramatic decrease in the splash criteria, mainly represented by the critical Reynolds number. Splash criteria showed more sensitivity to roughness ratio at low values of roughness and it became almost insensitive to roughness changes at high values of surface roughness ratio.

- The highest achievable Reynolds number for deposition was lower than 400 (happened for impaction on smooth surface). All the Newtonian liquid jets having Reynolds numbers higher than 400 ended in splash for all different surfaces.

4.2 Conclusions for Elastic Jet Impaction

- Complete analysis of jet impaction for twelve different solutions of polyethylenoxide (PEO) and water on one smooth and one rough surface suggested that elasticity will help to increase the splash threshold. Liquid jet depositions even happened at Reynolds number around 2000.

- Similar to the Newtonian liquid jet impaction, Weber number and jet relative angle were not playing an important role in determining splash. Reynolds and Deborah number

were the two important parameters in determining splash onset for elastic liquid jet impaction.

- In cases of splash for elastic liquids, much larger post impact droplets were observed in comparison with splash happening in Newtonian liquids. The elastic post impact droplets were also connected to each other by thin liquid ligaments. The existing elastic forces within these liquids can be responsible for this behaviour.

4.3 Recommendations for Future Works

Studies of Newtonian and elastic liquid jet impaction on a moving surface showed promising results for designing an industrial airless sprayer. The accomplished experiments showed that increased transfer efficiency and simplicity of design and carriage can be hoped as the main benefits of airless sprayers over the old atomization systems. Simple chemical changes can be suggested in the industrial LFM solution in order to avoid the splash, like increasing the viscosity and elasticity of the liquid. Results also insure that surface tension of the LFM is not an effective parameter for chemical improvements of the liquid.

Some interesting academic questions arise from of the current project. Some of the most important ones are:

- The current set-up can not exactly replicate the effects of cross wind and associated boundary layer effects that may happen in the field for the impacting rail surface. A more elaborate experimental set up can be designed for the purpose of studying the effects of crosswinds and moving surface boundary layer on the splash. These effects can be much more significant in high speed applications.

- The effect of Weber number on jet splash at low range of Weber numbers has not been studied. The current nozzle geometry did not allow us to test Weber numbers lower than 100 and the effects of Weber number in that range may be more significant. Making smaller nozzles which can provide lower speeds and consequently lower Weber numbers can shed some more light on this issue.

- From a number of different non-Newtonian behaviours, only one, elasticity, was selected and tested due to its dominant effect for droplet impact which was mentioned in the literature. However, several other effects such as yield stress, shear thinning/thickening remain untouched. Further studies in these areas may give alternative suggestions for splash inhibition other than adding elasticity.

- Due to upsurge interest in high speed trains, further studies for the application of the same airless nozzle for higher train/jet speeds can be an interesting field for both industrial and academic challenges.

Bibliography

[1] Cotter, J., Eadie, D.T., Elvidge, D., Hooper, N., Robert, J., Makowsky, T., and Liu, Y., 2005. Top of Rail Friction Control : Reductions in Fuel and Greenhouse Gas Emissions. In: Proc. Of the 2005 Conference of the International Heavy Haul Association (Rio de Janeiro), pp. 327-334.

[2] Li, L.K.B., Dressler, D.M., Green, S.I., Davy, M.H., and Eadie, D.T., 2009. Experiments on Air-Blast Atomization of Viscoelastic Liquids, Part 1: quiescent Conditions. Journal of Atomization and Sprays, 19:157-190.

[3] Dressler, D.M., Li, L.K.B., Green, S.I., Davy, M.H., and Eadie, D.T., 2009. Newtonian and Non-Newtonian Spray Interaction with a High-Speed Moving Surface. Journal of Atomization and Sprays, 19:19-39.

[4] Li, L.K.B., Green, S.I., Davy, M.H., and Eadie, D.T., 2010, Air-blast atomization of viscoelastic liquids in a cross-flow, Part 1: Spray Penetration and Dispersion, accepted for publication in Journal of Atomization and Sprays.

[5] Li, L.K.B., Green, S.I., Davy, M., and Eadie, D.T., 2010, Air-blast atomization of viscoelastic liquids in a cross-flow, Part 2: Droplet velocities, accepted for publication in Journal of Atomization and Sprays.

[6] Rein, M., 1993, Phenomena of Liquid Drop Impact on Solid and Liquid Surfaces, Fluid Dynamics Research, 12:61-93.

[7] Rioboo, R., Marengo, and M., Tropea, C, 2002, Time Evolution of Liquid Drop Impact onto Solid, Dry Surfaces, Experiments in Fluids, 33:112-124.

[8] Yarin, A.L., 2006, Drop Impact Dynamics: Splashing, Spreading, Receding, Bouncing…, Annual Review of Fluid Mechanics, 38:159-192.

[9] Deegan, R.D., Brunet, P., and Eggers, J., 2008, Complexities of Splashing, Nonlinearity, 21:1-11.

[10] Range, K., and Feuillebois, F., 1998, Influence of Surface Roughness on Liquid Drop Impact, Journal of Colloid and interface Science, 203:16-30.

[11] Bergeron, V., Bonn, D., Martin, J. Y., and Vovelle, L., 2000, Controlling Droplet Deposition with Polymer additives, Nature, 405:772-775

[12] Mundo, C., Sommerfield, M., and Tropea, C., 1995, Droplet-Wall Collisions: Experimental Studies of the Deformation and Breakup Process, International Journal of Multiphase Flow, 21:151-173.

[13] Povarov, O.A., Nazarov, O.I., Ignat'evskaya, L.A., and Nikol'Skii, A.I., 1976, Interaction of drops with boundary layer on rotating surface, Journal of Engineering Physics, 31:1453-1456.

[14] Courbin, L., Bird, J.C., and Stone, H.A., 2006, Splash and anti-Splash: Observation and Design., Chaos, 16:041102.

[15] Bird, J. C., Tsai, S.S.H., and Stone, H.A., 2009, Inclined to Splash: Triggering and Inhibiting a Splash with Tangential Velocity, New Journal of Physics, 11 :1 -6(2009).

[16] Ruiter, J. D., Pepper, R.E., and Stone, H.A., 2010, Thickness of the Rim of an Expanding Lamella Near the Splash Threshold, Physics of Fluids, 22:1-9.

[17] Okawa, T., Shiraishi, T., and Mori, T., 2008, Effect of impingement angle on the outcome of single drop impact onto a plane water surface, Experiments in Fluids, 44:331-339.

[18] Fathi, S., Dickens, P., and Fouchal, F., 2010, Regimes of droplet train impact on a moving surface in an additive manufacturing process, Journal of Material Processing Technology, 210:550-559.

[19] Dressler, D.M., 2006, An experimental investigation of Newtonian and non-Newtonian spray interaction with a moving surface, M.A.Sc. Thesis, UBC.

[20] Liu, X., and Lienhard V, J.H., 1993, The Hydraulic Jump in Circular Liquid Impingement and in Other Thin Films, Experiments in Fluids, 15:108-116.

[21] Hlod, A., AArts, A.C.T., van de Ven, A.A.F., and Peletier, M.A., 2007, Mathematical model of falling of a viscous jet onto a moving surface, European Journal of Applied Mathematics, 18:659-677.

[22] Lefebvre, A.W., *Atomization and Sprays*, Hemisphere Publishing Corporation, 1989, p. 159.

[23] Suh, H. K., Park, S.H., and Lee, C.S., 2008, Experimental investigation of nozzle cavitating flow characteristics for diesel and biodiesel fuels, International Journal of Automotive Technology, 9:217-224.

[24] Payri, R., Guadiola, C., Salvador, F.J., and Gimeno, J., 2006, Critical Cavitation Number Determination in Diesel Injection Nozzles, Experimental Techniques, 28:49-52.

[25] Middleman, S., and Gavis, J., 1961, Expansion and Contraction of Capillary Jets of Newtonian Liquids, Physics of Fluids, 4:355-359.

[26] Middleman, S., *Modeling Axisymmetric Flows*, Academic Press, 1995, p. 79.

[27] Crooks, R., and Boger, V., 2000, Influence of fluid elasticity on drops impacting on dry surfaces, Journal of Rheology, 44:973-996.

[28] Roux, D. C., Cooper-White, J. J., McKinley,G. H., and Tirtaatmadja, V.,2003, Drop Impact of Newtonian and Elastic Fluid, Physics of Fluids, 15:S12,

[29] Keshavarz, B., Green, S. I., Davy, M. H., and Eadie, D. T., 2010, Newtonian liquid jet impaction on a high speed moving surface, submitted to International Journal of Heat and Fluid Flow.

[30] Doi, M., and Edwards, S., F., 1999, Theory of Polymer Dynamics, Oxford University Press

[31] Boger, D. V., 1987, Visco-elastic flows through contractions, Annual Review of Fluid Mechanics, 19:157-182

[32] Boger, D. V., and Walters, K., 2000, Experimental dilemmas in non-Newtonian fluid Mechanics and their theoretical resolution, Korea-Australia Rheology Journal, 12:27-38.

[33] Rothstein, J., and McKinley, G. H., 2001, The Axisymmetric contraction-expansion: the role of extensional rheometry on vortex growth dynamics and the enhanced pressure drop, Journal of non-Newtonian Fluid Mechanics, 98:33-63

[34] Cartalos, U., and Piau, J. M., 1992, Creeping flow regimes of low concentration polymer solutions in thick solvents through an orifice die, Journal of non-Newtonian Fluid Mechanics, 45:231-285

[35] Eadie, D.T., Bovey, E., and Kalousek, J., 2002, The role of friction control in effective management of the wheel/rail interface, Railway Technical Conference, November 2002.

[36] Eadie, D.T., and Kalousek, J., 2001, Spray it on, Let'em Roll, Railway Age.

Appendix A: Splash/Deposition Results of Newtonian Liquids Impaction on Rough Surfaces

Splash and deposition results for Newtonian liquid jet impaction on four other tested rough surfaces are shown in this appendix. Figures 26, 27, 28, 29, 30, 31, 32, and 33 are showing the mentioned results in terms of related dimensionless numbers.

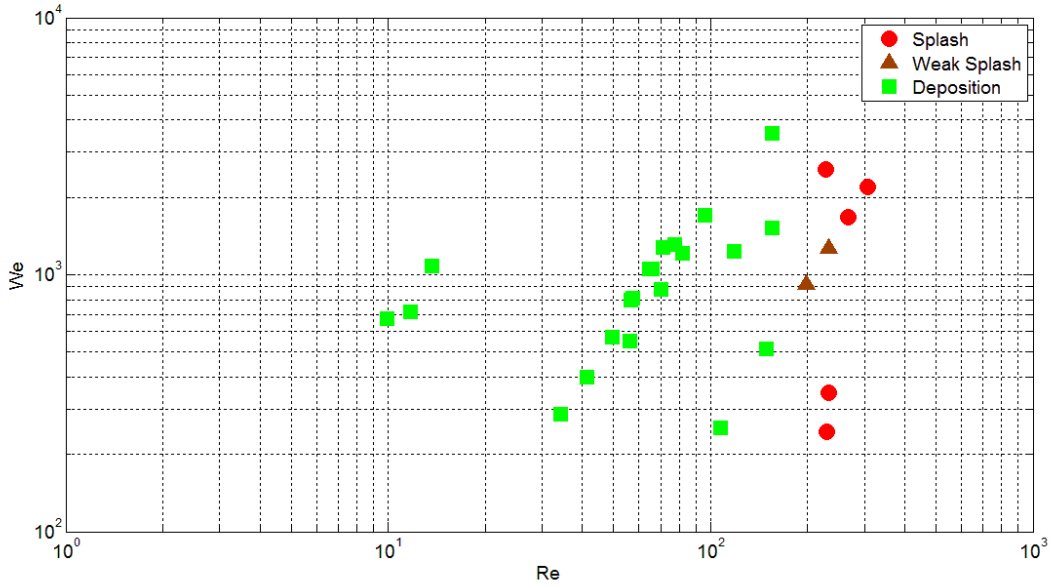

Figure 26: Splash/non-Splash results for impact of Newtonian liquids on a surface with roughness ratio equal to 0.02 (We vs. Re)

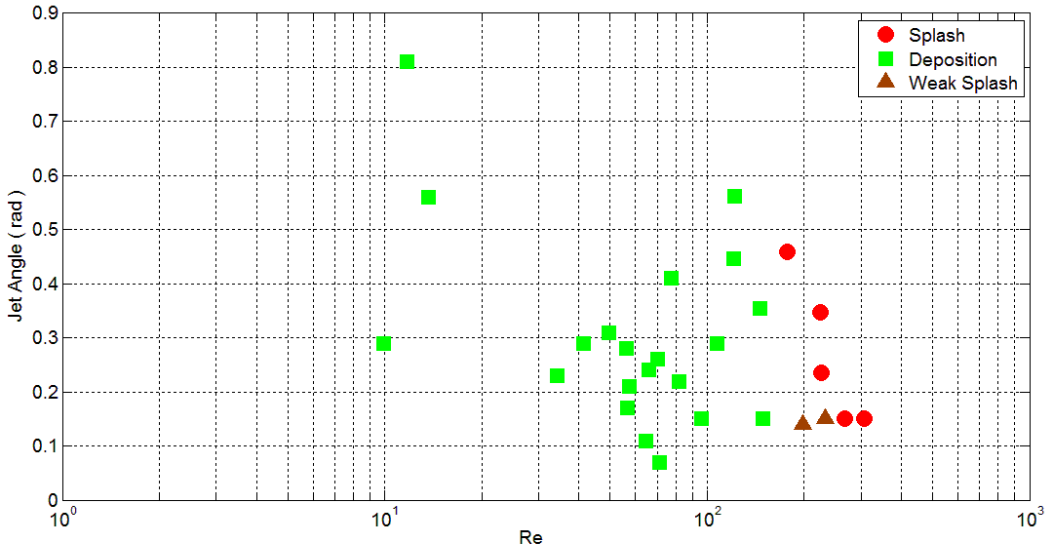

Figure 27: Splash/non-Splash results for impact of Newtonian liquids on a surface with roughness ratio equal to 0.02 (Jet Angle vs. Re)

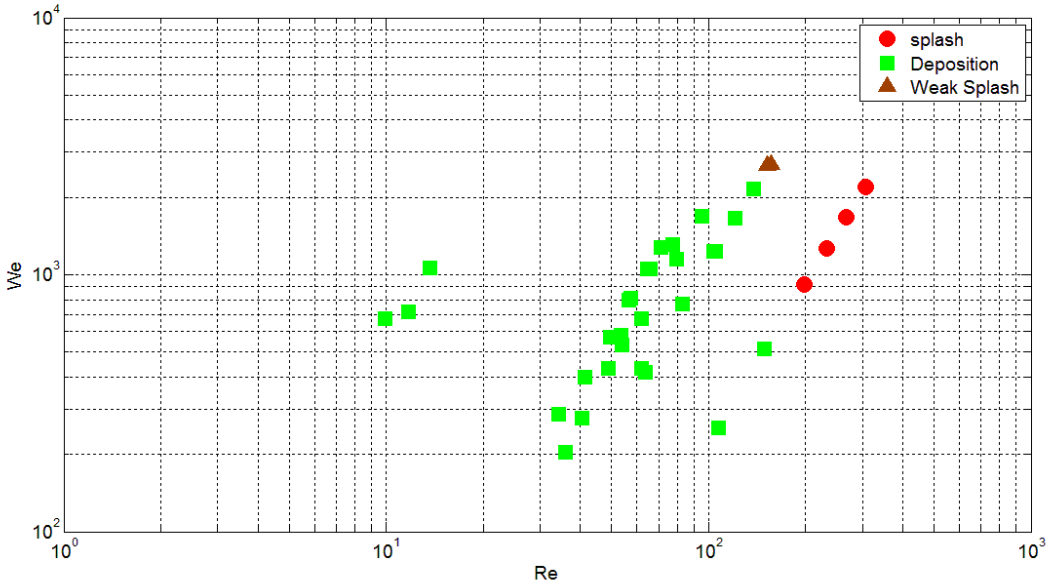

Figure 28: Splash/non-Splash results for impact of Newtonian liquids on a surface with roughness ratio equal to 0.1 (We vs. Re)

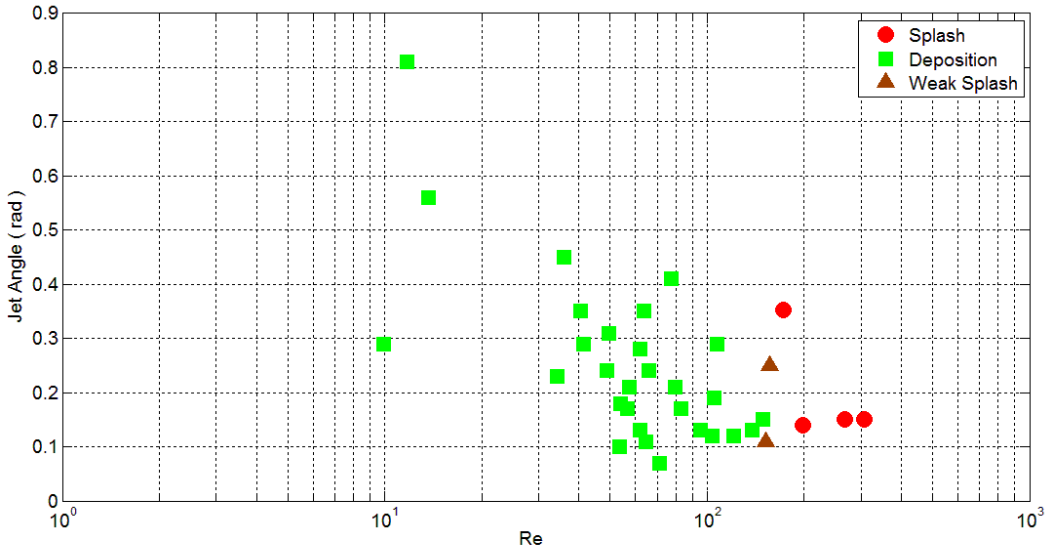

Figure 29: Splash/non-Splash results for impact of Newtonian liquids on a surface with roughness ratio equal to 0.1 (Jet Angle vs. Re)

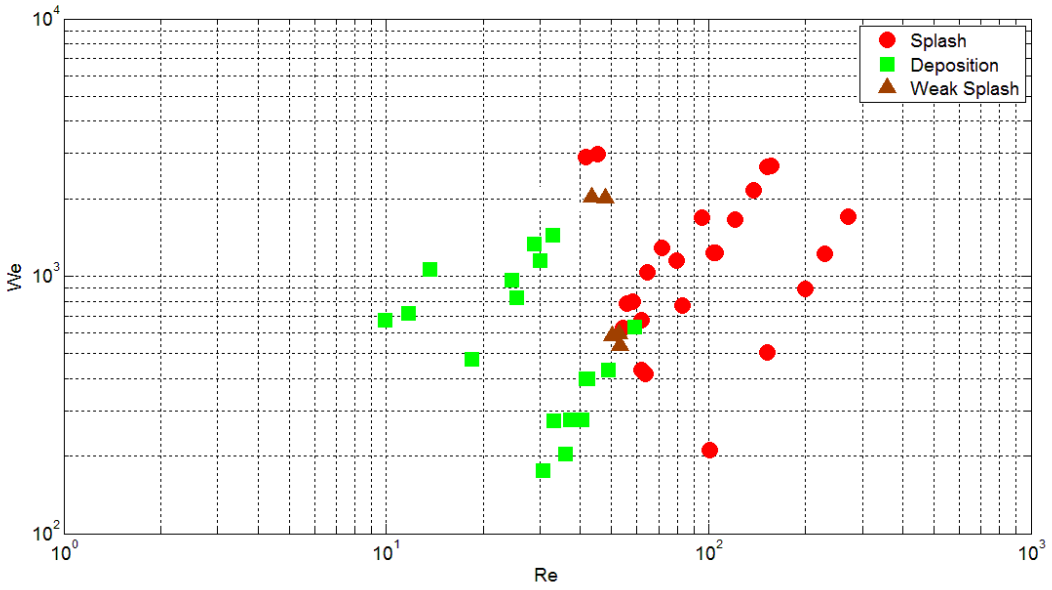

Figure 30: Splash/non-Splash results for impact of Newtonian liquids on a surface with roughness ratio equal to 0.41 (We vs. Re)

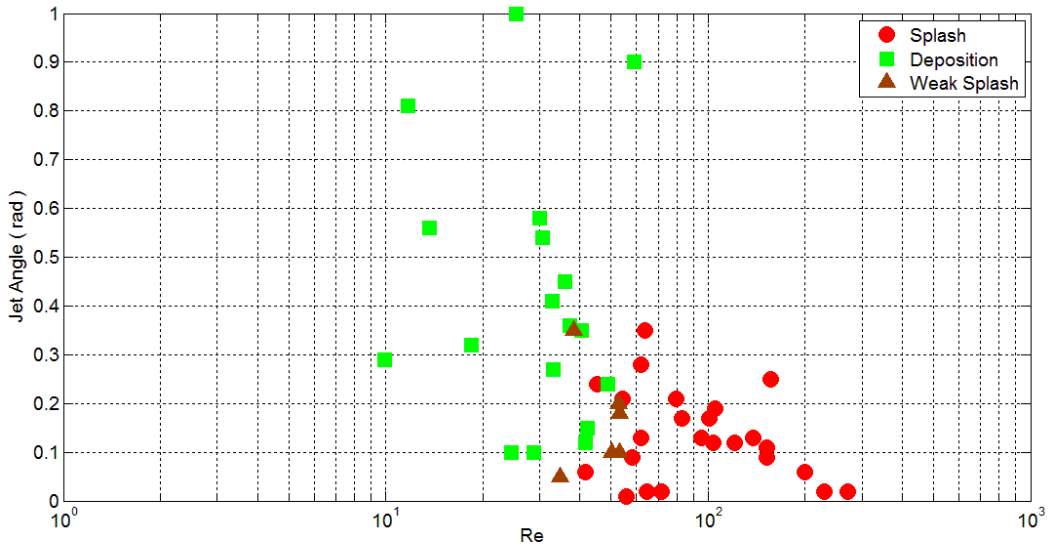

Figure 31: Splash/non-Splash results for impact of Newtonian liquids on a surface with roughness ratio equal to 0.41 (Jet angle vs. Re)

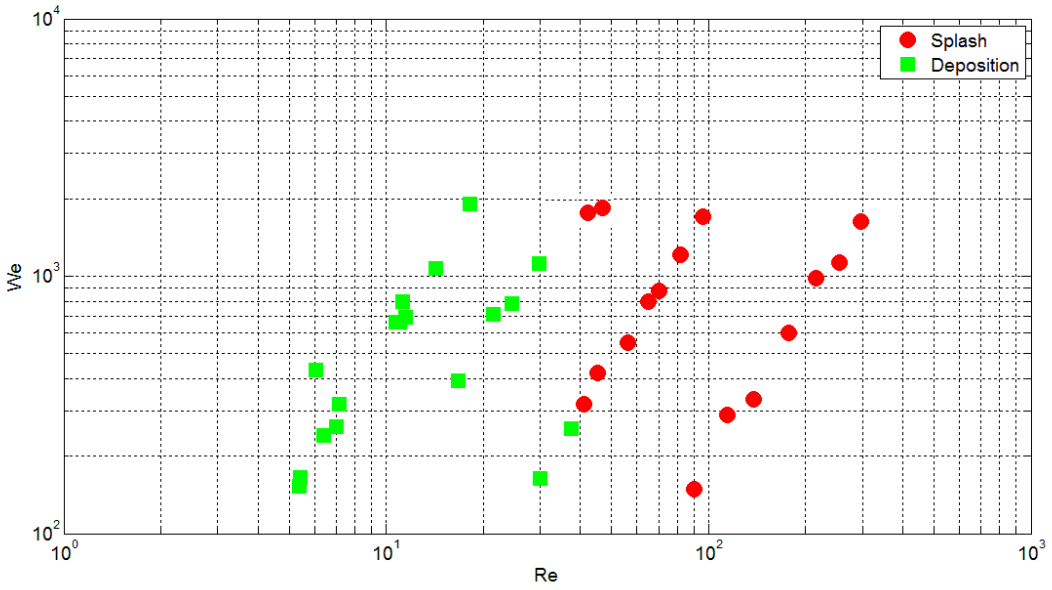

Figure 32: Splash/non-Splash results for impact of Newtonian liquids on a surface with roughness ratio equal to 0.65 (We vs. Re)

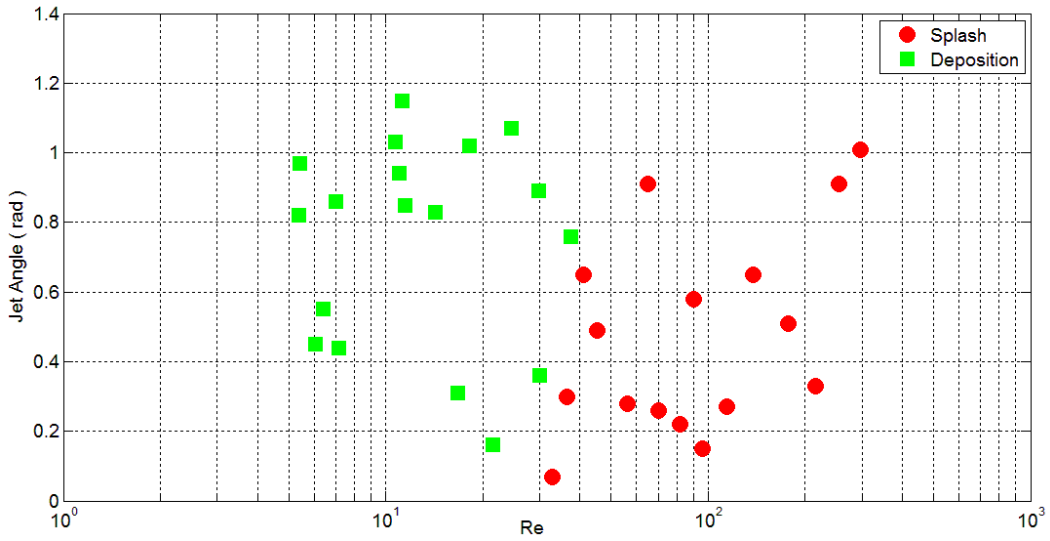

Figure 33: Splash/non-Splash results for impact of Newtonian liquids on a surface with roughness ratio equal to 0.65 (Jet angle vs. Re)